The EMBO Journal (2013) 32, 2920–2937
www.embojournal.org

TRANSPARENT PROCESS

THE EMBO JOURNAL

Amyloid-β oligomers induce synaptic damage via Tau-dependent microtubule severing by TTLL6 and spastin

Hans Zempel[1], Julia Luedtke[1,2], Yatender Kumar[1,2], Jacek Biernat[1], Hana Dawson[3], Eckhard Mandelkow[1,2,4] and Eva-Maria Mandelkow[1,2,4,*]

[1]DZNE, German Center for Neurodegenerative Diseases, Bonn, Germany, [2]MPI for Neurological Research, Hamburg Outstation, Hamburg, Germany, [3]Duke University Medical Center, Durham, NC, USA and [4]CAESAR Research Center, Bonn, Germany

Mislocalization and aggregation of Aβ and Tau combined with loss of synapses and microtubules (MTs) are hallmarks of Alzheimer disease. We exposed mature primary neurons to Aβ oligomers and analysed changes in the Tau/MT system. MT breakdown occurs in dendrites invaded by Tau (Tau missorting) and is mediated by spastin, an MT-severing enzyme. Spastin is recruited by MT polyglutamylation, induced by Tau missorting triggered translocalization of TTLL6 (Tubulin-Tyrosine-Ligase-Like-6) into dendrites. Consequences are spine loss and mitochondria and neurofilament mislocalization. Missorted Tau is not axonally derived, as shown by axonal retention of photoconvertible Dendra2-Tau, but newly synthesized. Recovery from Aβ insult occurs after Aβ oligomers lose their toxicity and requires the kinase MARK (Microtubule-Affinity-Regulating-Kinase). In neurons derived from Tau-knockout mice, MTs and synapses are resistant to Aβ toxicity because TTLL6 mislocalization and MT polyglutamylation are prevented; hence no spastin recruitment and no MT breakdown occur, enabling faster recovery. Reintroduction of Tau re-establishes Aβ-induced toxicity in TauKO neurons, which requires phosphorylation of Tau's KXGS motifs. Transgenic mice overexpressing Tau show TTLL6 translocalization into dendrites and decreased MT stability. The results provide a rationale for MT stabilization as a therapeutic approach.

The EMBO Journal (2013) **32,** 2920–2937. doi:10.1038/emboj.2013.207; Published online 24 September 2013
Subject Categories: neuroscience
Keywords: Abeta-oligomers; spastin; Tau missorting; MARK/par-1; Alzheimer disease

Introduction

Alzheimer disease (AD) is characterized by two types of abnormal protein aggregates in the brain, 'amyloid plaques' made up of Aβ peptides, and 'neurofibrillary tangles' assembled from Tau protein (Mandelkow and Mandelkow, 2012; Mucke and Selkoe, 2012). In familial AD, genetic evidence points to a master role of Aβ aggregation, leading to downstream events including Tau hyperphosphorylation and aggregation (Haass and Selkoe, 2007; Karran *et al*, 2011). On the other hand, the distribution of Tau aggregates in the brain correlates better with the clinical progression of AD (Braak stages; Braak and Braak, 1991), and experiments with transgenic mice suggest a critical role for Tau in mediating Aβ-induced toxicity.

A key to understand the normal and toxic roles of Tau lies in the neuronal cytoskeleton, notably microtubules (MTs), the tracks of intracellular transport, and their interaction partners. Tau changes during development include (i) a shift from shorter fetal to longer adult isoforms, (ii) decreased phosphorylation (from a higher fetal to a lower adult level), and (iii) changed intracellular distribution (from ubiquitous to axonal) (Mandell and Banker, 1995; Bullmann *et al*, 2009). Notably, the early cytoskeletal changes in AD, such as lower MT stability, hyperphosphorylation, and missorting of Tau to the somatodendritic compartment, are reminiscent of the fetal state. In TauKO mice, the lack of Tau during development can be compensated by upregulation of other neuronal microtubule associated proteins (MAPs), for example, MAP1A (Harada *et al*, 1994), which may explain the mild phenotype. Depending on experimental conditions, the absence of Tau may have detrimental effects (inefficient axon outgrowth and neurodegeneration; Dawson *et al*, 2001; Dawson *et al*, 2010), or beneficial ones (reduction in Aβ and excitotoxicity; King *et al*, 2006; Roberson *et al*, 2007; Ittner *et al*, 2010). In neuronal cell culture, excess Tau leads to inhibition of axonal transport (Stamer *et al*, 2002), and aggregation of mutant Tau in mouse models causes Alzheimer-like degeneration (Sydow *et al*, 2011).

Neurons must possess mechanisms to modulate MT stability. This includes 'dynamic instability' of MTs, which is controlled by regulatory proteins. Some of these, for example MAPs, can stabilize MTs depending on their phosphorylation; kinases such as MARK (Microtubule-Affinity-Regulating-Kinase) can phosphorylate Tau and other MAPs, detaching them from MTs, thereby rendering MTs more dynamic (Matenia and Mandelkow, 2009). Other enzymes can sever MTs, induce their endwise disassembly, or control the supply of tubulin subunits (Baas *et al*, 2005; Conde and Caceres, 2009; Hoogenraad and Bradke, 2009). These are active processes requiring energy (ATP) and depend on spatial and temporal cues, for example by post-translational modifications of the MT surface (Janke and Kneussel, 2010).

In the current study, we set out to determine a mechanistic link between Aβ exposure, Tau missorting, and MT breakdown. We show that Aβ causes Tau missorting and consequent Tubulin-Tyrosine-Ligase-Like-6 (TTLL6) mislocalization. TTLL6 induces polyglutamylation of MTs, which then allows recruitment and severing by spastin. The result is

*Corresponding author. DZNE, German Center for Neurodegenerative Diseases, Ludwig-Erhard-Allee 2, Bonn 53175, Germany.
Tel.: +49 228 43302 630; Fax: +49 228 43302 689;
E-mail: mandelkow@mpasmb.desy.de

Received: 15 July 2013; accepted: 22 August 2013; published online: 24 September 2013

©2013 European Molecular Biology Organization

a perturbation of MT-based traffic, especially of mitochondria. This cascade is reversible because Aβ oligomers (AβOs) lose their toxic potential with time, allowing Tau to resume a polar distribution and regrowth of spines. In neurons from TauKO mice, Aβ-induced toxicity is greatly reduced, supporting the view that Tau is a critical mediator of Aβ-induced neurodegeneration. The toxic function of Tau following Aβ exposure can be re-established in Tau-KO neurons by re-introducing wild-type Tau or phospho-mimicking forms of Tau, but not of non-phosphorylatable variants, indicating an essential role for phosphorylation in the toxic cascade.

Results

Time slicing of cytoskeletal changes induced by AβOs

AβOs are capable of inducing Tau missorting in primary neurons, which is accompanied by Ca^{++} elevation, loss of MTs, loss of spines, and phosphorylation of Tau at the KXGS motifs in the repeat domain (Zempel *et al*, 2010). Here, we employed a more potent preparation of AβOs that reflects the composition of Aβ in Alzheimer brain (70% $Aβ_{40}$ and 30% $Aβ_{42}$; Kuperstein *et al*, 2010, see Supplementary Results and Supplementary Figures S1 and S2). The preparation was composed of tri- and tetramers when analysed by SDS–PAGE, was positive for an oligomer-specific antibody (A11 antibody by C Glabe: recognizes oligomers in a dot blot setting), and revealed aggregates of 5–25 nm size but no fibrils by negative stain electron microscopy (Supplementary Figure S1a–e). We evaluated effects of AβOs by quantifying the level of changes in the dendritic compartments (preselected by MAP2), the areas affected by Tau missorting.

When challenging neurons with 1 μM AβOs, Tau missorting into the somatodendritic compartment becomes apparent, but only for a limited time (1–12 h), with a maximum around 3–6 h, and then gradually reverts to background levels after 24 h (Figure 1A, arrows; Figure 1F), despite the continued presence of Aβ (as AβOs loses their toxicity over time, see below).

To clarify the time course of events leading to the phosphorylation of missorted Tau, we tested the activity of MARK using an antibody against its phosphorylated T-loop (pT208), since MARK is the most important regulator for Tau affinity to MTs via phosphorylation of Tau at the KXGS motifs (Matenia and Mandelkow, 2009). Following exposure to AβOs, we found increased activation of MARK in the somatodendritic compartment, lagging behind the missorting of Tau (Figure 1F), but there was no activation of MARK in the axonal compartment (Figure 1B; Supplementary Figure S3). Likewise, the increase in MARK-induced phosphorylation of Tau at KXGS motifs (S262/S356, detected by antibody 12E8) occurred with a similar time course, lagging behind total missorted Tau (Figure 1F). Thus, the delayed and locally restricted activation of MARK suggests that MARK activation and Tau phosphorylation are not the primary cause of Tau missorting.

We next tested whether we could induce Tau missorting independently of kinase activation. Very brief exposure to the MT destabilizer nocodazole (10 μM) or elevated concentrations of Ca^{++} in the medium (5 mM) resulted in fast missorting of Tau (i.e., starting at 15 min, 4 × faster than with AβOs) (Supplementary Figure S4a). Such rapid missorting of Tau was not accompanied by phosphorylation in the repeat domain, which did not appear even at later time points (Supplementary Figure S4a). Thus, Tau missorting can occur without activation of MARK and without phosphorylation in Tau's repeat domain.

We then tried to dissect the temporal sequence of these events. Several studies have shown that exposure to Aβ initially causes rapid changes (within minutes) in neuronal signalling, visible in terms of electrical activity and Ca^{++} oscillations (Snyder *et al*, 2005; Rui *et al*, 2006). Superimposed on this we observed a gradual rise in intracellular Ca^{++} from basal levels (~0.2 μM) by about 50–100%, peaking ~1 h after exposure to Aβ (Figure 1D) and visible up to 6 h. This rise in Ca^{++} was accompanied by a decrease in MTs (~40%) in dendrites, but not axons, and reduction in dendritic spines (~40%). These changes reverted by 12 h and remained steady up to 24 h (Figure 1C–F). The rise in Ca^{++} and decrease in MTs and spines occurred roughly in parallel with the increase in missorted Tau; however, Tau phosphorylation and MARK activation were delayed by ~1 h. This suggests that loss of dendritic MTs and spines occurs by a mechanism not directly caused by phosphorylation of Tau in the repeat domain. Dendritic Tau also returned to its basal level, but much more slowly (up to 24 h).

Aβ-induced Ca^{++} elevation depended on Ca^{++} influx from the extracellular medium. Chelation of extracellular Ca^{++} by EGTA (0.5 mM), and of intracellular Ca^{++} by BAPTA-AM (10 μM) prevented Tau missorting and loss of MTs, but also caused toxic side effects such as severe spine loss, likely due to impaired Ca^{++} homeostasis (Higley and Sabatini, 2008). Increase in intracellular Ca^{++} was completely and rapidly (<3 min) reversible even when Ca^{++} was chelated after incubation with Aβ (20 min and 1 h after AβO exposure, before Ca^{++} started to decrease, see above). This indicates that extracellular Ca^{++} is necessary for the rise and the maintenance of elevated Ca^{++} in response to AβOs.

Two further changes are indicative of Aβ-induced MT loss: clustering of mitochondria in the cell body was observed from 1 to 6 h (Figure 1D, see also below), suggesting impaired MT-dependent transport (Stamer *et al*, 2002). Neurofilaments (which are normally transported into axons) accumulated in the soma upon Aβ exposure and then invaded dendrites (peak time after 3–6 h; Supplementary Figure S4b). Similarly to Tau, the missorting of neurofilaments started to reverse as soon as MT loss is reversed (i.e., after 6 h).

AβOs induce polyglutamylation of MTs, causing the recruitment of spastin for MT severing

Post-translational modifications of MTs are well-known indicators of MT stability and interactions. When testing these in dendritic MTs, we observed a sharp drop in acetylation, which represents 'old' stable MTs, with little change in the more dynamic tyrosinated MTs (Figure 2A and B) (Janke and Kneussel, 2010). Other important MT destabilizing proteins are katanin and spastin (Roll-Mecak and McNally, 2010). There was no Aβ-induced change in katanin subunit p60 and p80 levels or localization, and knockdown of katanin had no effect (Supplementary Figure S5). Loss of MAP2 (the major MAP in dendrites) might account for destabilization of dendritic MTs, but MAP2 levels were not decreased

©2013 European Molecular Biology Organization

(Supplementary Figure S6a and b; Supplementary Results). However, spastin was noticeably recruited to MTs after AβO exposure (Figure 2C), suggesting that spastin is responsible for MT loss.

To verify this, we reduced the expression of spastin via shRNA (Riano *et al*, 2009). Knockdown of spastin abolished Aβ-induced MT loss, and likewise prevented Tau missorting (Figure 2D; Supplementary Figure S7a–c). Scrambled control

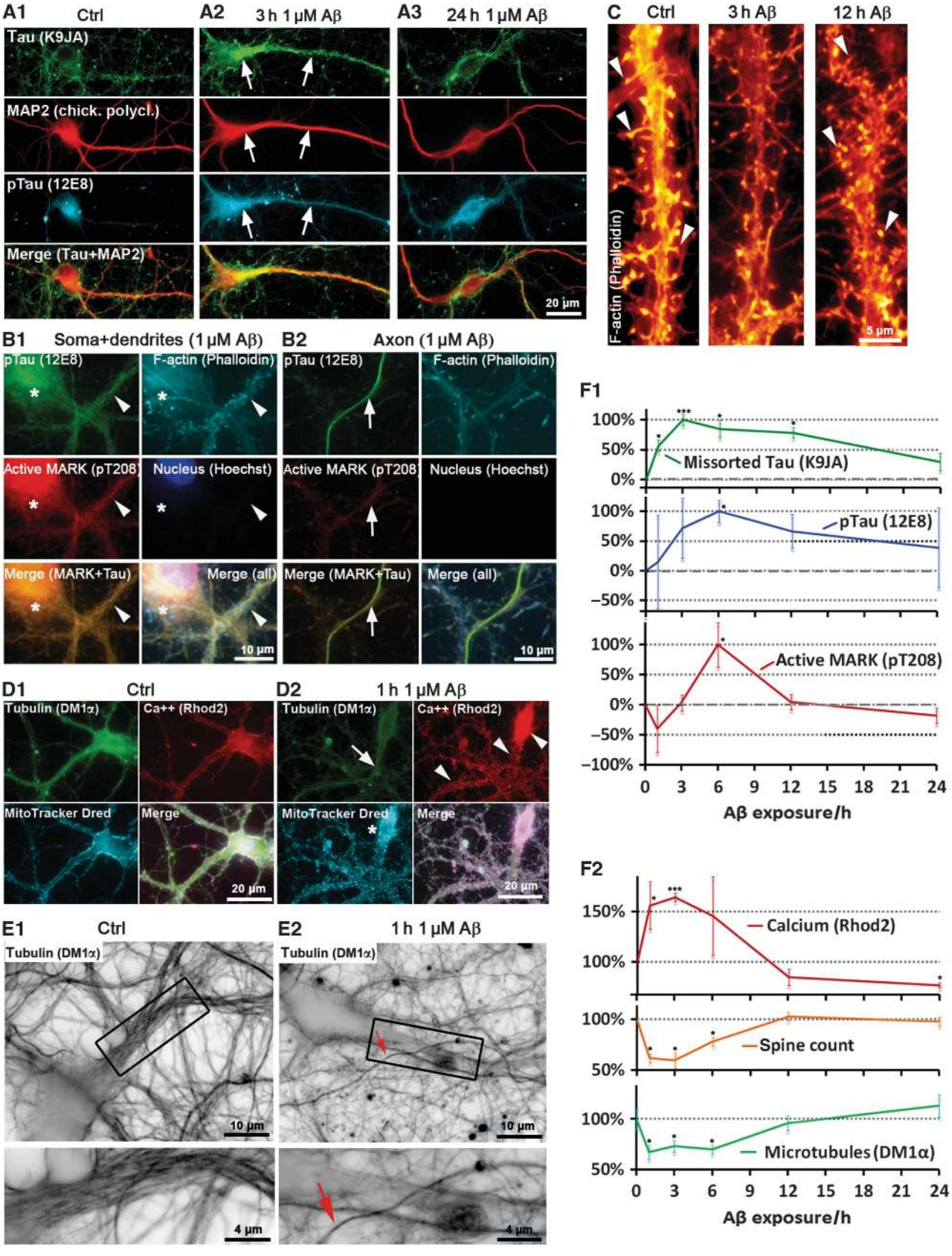

©2013 European Molecular Biology Organization

shRNA or the empty vector had no effect. Spastin is known to be recruited by polyglutamylation, a post-translational modification of MTs (Lacroix *et al*, 2010). Indeed, we observed a pronounced increase in polyglutamylated MTs (~2-fold) in response to AβOs, consistent with the attachment of spastin to MTs and MT severing (Figure 2B–D).

Polyglutamylation is induced by the TTLL family of tyrosine ligases, TTLL6 being the main enzyme responsible for polyglutamylation that leads to MT severing (Lacroix *et al*, 2010). We found that this protein is recruited to MTs and colocalizes with sites of increased polyglutamylation in dendrites suffering from strong Tau missorting after AβO exposure (Figure 3A and B). Conversely, transfection of TTLL6 leads to strong polyglutamylation of MTs, heavy spastin recruitment, breakdown of MTs, and Tau missorting (Figure 3C) even in the absence of AβOs. All of these features suggest that the loss of MTs after AβO exposure is caused by polyglutamylation of MTs by TTLL6, followed by recruitment of spastin and then severing.

Missorted Tau in dendrites is not derived from axons but is newly synthesized

The mechanisms of Tau's axonal sorting are still only partly understood, but important for understanding AD because somatodendritic missorting is an early indicator of neurodegeneration (Braak *et al*, 1994). Axonal retention of Tau is achieved in part by a diffusion barrier located at the axon initial segment (AIS) (Li *et al*, 2011). We asked whether this barrier remains intact or breaks down after exposure to AβOs. The detection system makes use of the photoconversion of Dendra2-tagged hTau40 (Tau^{D2}) transfected into mature neurons. This reveals that axonal Tau does not re-enter the somatodendritic compartment under control conditions (Figure 4A1). The barrier can be broken down by disassembly of axonal MTs (e.g., by nocodazole; Figure 4A3). By contrast, exposure of neurons to AβOs did not enable axonal Tau^{D2} to propagate back into the soma since the barrier remained intact (Figure 4A and B). The expression of Tau^{D2} did not interfere with the targeting of Aβ to dendritic spines (Figure 4C). This argues that Tau missorted into the somatodendritic compartment is not derived from translocated axonal Tau.

To clarify this issue, protein synthesis was inhibited with cycloheximide (Figure 4D). This treatment suppressed missorting of endogeneous Tau by AβOs. Since cycloheximide might affect other processes important for maintenance of Tau polarity, we used shRNA against Tau as a further control. As soon as expression (via co-transfection of GFP-derivative tdTomato) was detectable (17 h post transfection), cells were challenged with AβOs. While co-transfected tdTomato alone did not prevent missorting, shRNA against Tau prevented AβO-induced missorting of Tau (Supplementary Figure S7d). Thus, the inhibition of both global protein translation and specific early Tau protein translation confirms the conclusion that missorted Tau originates from Tau newly synthesized in the cell body.

Neurons and spines recover from Aβ-induced toxic effects

A remarkable feature of the Aβ-induced cell insults is their recovery: most effects are visible for only a few hours and return to their initial values after 12–24 h in our conditions. Several explanations are conceivable: cells could become resistant, or Aβ might lose its toxicity, due to chemical modification, degradation, or structural changes. Two consecutive hits with AβOs spaced several hours apart exacerbated spine loss but reduced Tau missorting (Figure 5A). Twenty-four hours after a single treatment with AβOs, spine numbers recovered to control levels, but after multiple hits (2–3) there was no recovery, indicating that cells did not become resistant to newly added AβO.

To test whether and how AβOs lose their toxicity, we incubated AβO (1 μM) for 3 h with or without cells. Both of these preincubated AβOs lost their toxicity to primary neurons, arguing that AβOs changed their properties with time independently of cells. In support of this, dynamic light scattering of AβOs diluted in PBS to 1 μM showed that within 3 h they transformed into larger and less toxic aggregates (Figure 5B and C), despite the fact that the process of aggregation can confer toxicity (Supplementary Figure S8, see also Wogulis *et al*, 2005; Kuperstein *et al*, 2010). We conclude that recovery of neurons takes place because the AβO preparation loses its toxicity, not because cells become less sensitive.

Of note, missorting of Tau is most pronounced after AβOs lose their toxicity, that is, after 3–6 h. When challenged repetitively at low intervals (3–6 h), missorting was not increased, but decreased. Furthermore, higher and more toxic concentrations of AβOs induced more severe spine

Figure 1 MARK activation triggers repolarization and spine recovery after Aβ-induced Tau missorting. Primary rat hippocampal neurons 21DIV were treated with 1 μM Aβ for different durations as indicated. (**A1**) Control cells show only background staining of Tau and very low phosphorylation of Tau at the KXGS motifs (12E8 epitope). (**A2**, **A3**) Cells treated with 1 μM Aβ. (**A2**) After 3 h of incubation, Tau is missorted into the somatodendritic compartment (arrows) and phosphorylated at the KXGS motifs. (**A3**) After 24 h of incubation, dendritic total Tau and p-Tau intensities decrease (quantification in **F1**). (**B**) Active MARK does not localize to axons. Cells were co-stained with antibodies against active MARK (pT208) and p-Tau (12E8), and with nuclear and F-actin stains. (**B1**) After exposure to Aβ (3 h, 1 μM), active MARK signals increase, but only in the somatodendritic compartment (quantified in **F1**; dendrite is indicated by arrowhead, cell body by star). (**B2**) Active MARK cannot be detected in axons (axon is indicated by arrows), in contrast to the somatodendritic compartment (compare **B2** and **B1**, left middle panels). (**C**) Spine loss is reversible; in control conditions (left panel) cells display a normal number of spines. After Aβ exposure for 3 h (middle panel), spines decay but grow back after 12 h (right panel). Arrowheads indicate spines, quantification in **F2**. (**D**, **E**) Cells were treated with 1 μM Aβ for 1 h. (**D1**) Control cells show dense packaging of MTs, homogeneously distributed mitochondria and low Ca^{++} levels. (**D2**) After treatment with Aβ (1 h, 1 μM), MTs depolymerize (dendrite indicated by arrow), Ca^{++} levels are elevated (arrowheads; quantified in **F2**), and mitochondria cluster in the soma (star). (**E**) MTs are lost in dendrites, but not in axons. (**E1**) Control cells display dense MTs in the dendrites (box: magnified in lower panel). (**E2**) After exposure to Aβ, dendritic MTs are lost (box: magnified in lower panel), whereas axonal MTs remain intact. Arrow indicates an axon crossing the dendrite. (**F1**) Changes in total Tau, pTau, and pMARK (**A**, **C**) revert to baseline after 12–24 h of treatment with Aβ. Dendritic increase in total Tau and pTau precede activation of MARK. (**F2**) Quantification of Ca^{++} and MT levels (**B**, **D**, **E**) in the proximal dendrites and spine count after different incubation times with 1 μM Aβ. Changes revert to baseline after 12–24 h of treatment. Rapid increases in Ca^{++} correlate with drop in MT and spine levels.

©2013 European Molecular Biology Organization

loss, but less missorting (data not shown). This indicates that neurons must still be 'viable' in order to generate Tau missorting, which likely depends on protein synthesis (see above), and is in line with previous results with other cell stressors that induced Tau missorting only when applied under relatively mild conditions (Zempel *et al*, 2010).

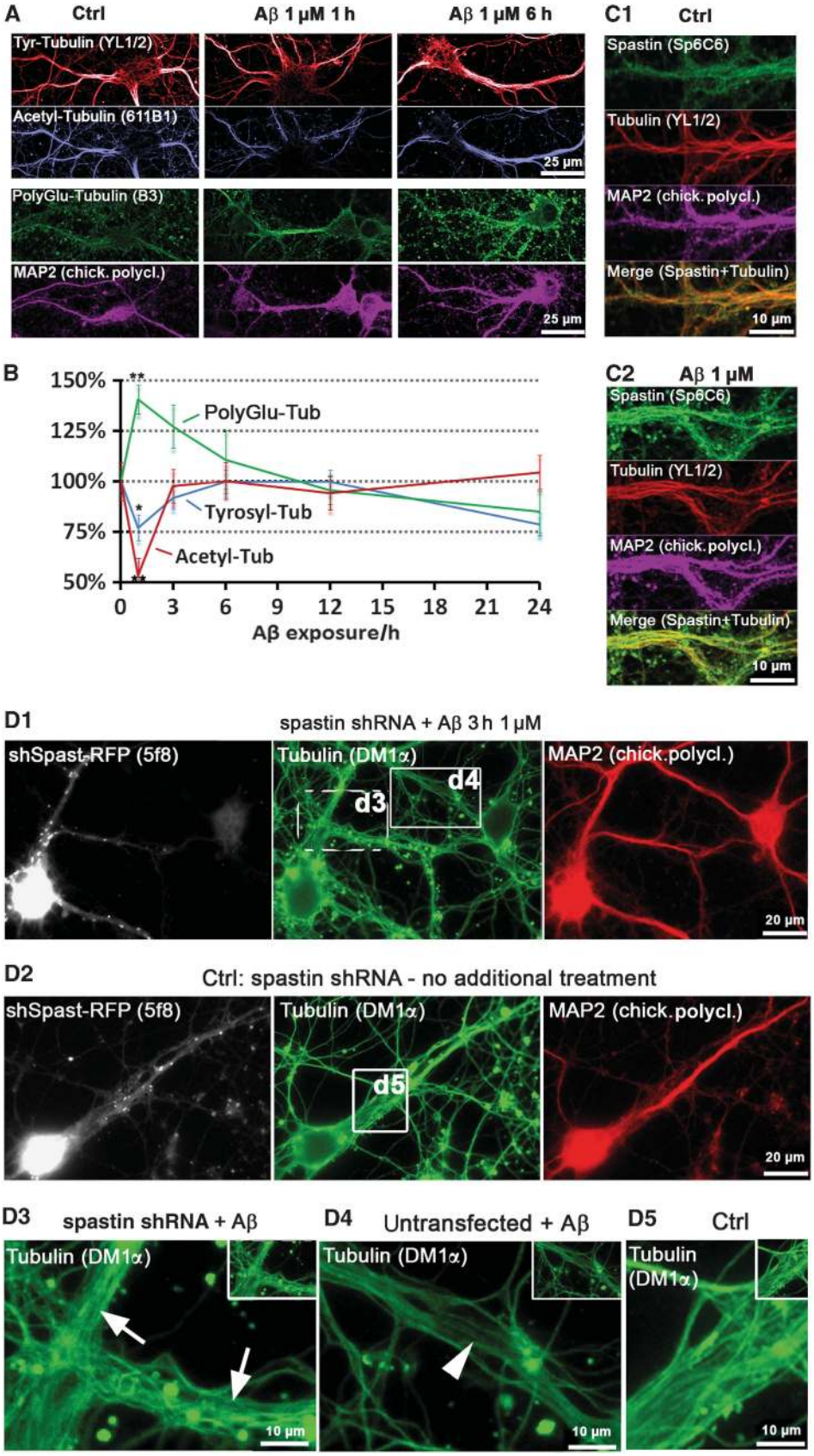

©2013 European Molecular Biology Organization

MARK re-establishes Tau polarity and restores spines during recovery from Aβ-induced toxicity

Kinases of the MARK/Par-1 family, in combination with other polarity genes, are known to be important for establishing cell polarity (Matenia and Mandelkow, 2009). MARK is activated in dynamic cell processes such as growth cones and dendritic spines (Hayashi *et al*, 2011; Timm *et al*, 2011), renders MT dynamic, and stabilizes the actin cytoskeleton (Matenia *et al*, 2005). MARK can phosphorylate Tau and detach it from MTs. Analysis of time courses after Aβ exposure (Figure 1F) revealed that Ca^{++} increase, MT decay, and spine loss are rapid (peaking within 1 h), total Tau missorting lags behind (peaking after 3 h), but activation of MARK takes place with a clear delay (peak at 6 h).

To test the role of MARK, we transfected wt-MARK2 by adenovirus 3 days prior to treatment with AβOs. Transfected MARK2 was sorted into the somatodendritic compartment and highly enriched in spines, where it colocalized with F-actin. Unexpectedly, the hallmarks of Aβ-induced toxicity disappeared, that is, spines remained stable, MTs did not decay, and there was no missorting of Tau into dendrites (Figure 5E1 and E2). Conversely, after treating cultures with the MARK-specific inhibitor compound 39 621 (Timm *et al*, 2011), we observed pronounced spine loss, with and without AβO exposure (Figure 5D), but no Tau missorting (Supplementary Figure S9). Furthermore, when applying the MT-stabilizer taxol (which prevents spine loss after Aβ insult, Figure 5D, and Tau missorting), we found upregulation of MARK activity and increased MARK-type Tau phosphorylation at the KXGS motifs, without changing total MARK levels (Figure 5F–H). Conversely, the MT-destabilizer nocodazole decreased MARK-type phosphorylation of Tau as well as MARK activity (Figure 5F and H).

Tau knockout neurons are resistant to AβO toxicity

There is an ongoing debate on the importance of Tau for neurons. Knockout of Tau in mice was reported to have only minor effects (Harada *et al*, 1994), to be detrimental (Dawson *et al*, 2010; Lei *et al*, 2012), or beneficial (Roberson *et al*, 2007; Ittner *et al*, 2010). We investigated how Tau deficiency in neurons from transgenic TauKO mice might change the response to AβOs. In TauKO neurons, the pathological changes were strongly reduced or absent, even though AβO was still targeted to dendrites and induced moderate spine loss (-15%, half of the effect in wild-type cells) (Figure 6A and B). In particular, in TauKO neurons, AβOs (1 μM) did not induce NF missorting, MT loss (Figure 6A–C), TTLL6 translocation into dendrites, polyglutamylation of MTs, and loss of acetylation of MTs, and spastin recruitment (Figure 7A–C and F, and see below). The Aβ-induced rise in steady-state Ca^{++} and MAP2 was lower in TauKO neurons (~20 and 50% of wild-type neurons, respectively; Figure 6A and B). Spastin was not recruited in TauKO neurons (Figure 7B).

TauKO neurons were also more resistant against other external challenges, such as elevated Ca^{++} (5 mM) or glutamate (10 μM) in the medium. In wild-type neurons, these concentrations would suffice to cause severe reduction in MTs, but in TauKO neurons they had no effect on dendritic MTs (Figure 6C), consistent with the reduced polyglutamylation in response to these stressors. Thus, MTs of TauKO neurons are better protected against depolymerization mediated by Aβ and other stressors that lead to an increase in intracellular Ca^{++}.

Since mitochondria travel along MTs, any loss of MTs would be expected to reduce the trafficking of mitochondria. Indeed, after exposure of wild-type neurons to AβOs, mitochondria were decreased in dendrites and clustered in cell bodies, while in TauKO neurons, mitochondria were evenly distributed and thus able to maintain spines and Ca^{++} buffering (Figure 6D). The localization of mitochondria to dendrites should result in faster recovery in TauKO neurons. Accordingly, synaptic activity (as measured by spontaneous Ca^{++} oscillations) was inhibited after AβO exposure in both wild-type and TauKO neurons, and fully recovered only in TauKO neurons, but not in wild-type cells (1 μM, 24 h; Supplementary Figure S10). This indicates that despite some recovery at the level of spines even in wild-type neurons (see above), rescue is either faster or more pronounced in TauKO cells.

Introduction of Tau re-sensitizes TauKO neurons to Aβ-induced spine loss and MT decay

We finally asked whether the introduction of Tau into hippocampal TauKO cells can re-sensitize them to AβO toxicity again. This was in fact observed: adenoviral transfection (for 3–4 days) of wild-type human Tau (hTau40) into TauKO neurons re-established Aβ-mediated Tau toxicity. Expression of Tau was sufficient to allow migration of TTLL6 from cell bodies into dendrites (Figure 7D). Exposure to Aβ caused spine loss similarly to wild-type cells. Accordingly, we also found pronounced polyglutamylation of MTs and spastin recruitment, resulting in MT severing, mislocalization of mitochondria and also observed elevated Ca^{++} (Figure 7E).

We then asked whether Tau missorting could also change TTLL6 localization in an *in vivo* model. In wild-type mice expressing only endogeneous mouse Tau, TTLL6 was concentrated in the soma and MTs were normally acetylated (Figure 7G1, left panels). In transgenic mice overexpressing a mutant form of hTau40 (Van der Jeugd *et al*, 2012), TTLL6 was translocated into the dendrites, and acetylation of MTs

Figure 2 Aβ exposure leads to rapid loss of acetylated, but not tyrosinated MTs, induces MT polyglutamylation and spastin recruitment in dendrites. Primary rat hippocampal neurons (16–21DIV) were treated with 1 μM Aβ as indicated, MAP2 staining was used as a marker for somatodendritic compartment. (**A**) In control cells, dendrites display high levels of tyrosinated and acetylated MTs, and low levels of polyglutamylated MTs. After short treatments (1 and 3 h), there is almost no change in tyrosinated MTs (upper panels), but a fast drop in acetylated MTs (middle panels). Polyglutamylation of MTs increases already after 1 h. Changes in all MT modifications are not observable anymore after 6 h of treatment (right panels). (**B**) Quantification of (**A**); changes revert to baseline after 6–12 h of treatment. (**C**) Cells were co-stained for spastin and MTs. (**C1**) Controls show only a diffuse spastin staining. (**C2**) After treatment with Aβ (1 μM, 3 h), spastin is recruited to MTs (increased colocalization with Tubulin in merge, lower panel). (**D**) Spastin was silenced using shRNA with a vector co-expressing RFP (5 days), cells were then treated with 1 μM Aβ for 3 h (**D1**, **D3**, **D4**) or left untreated (**D2**, **D5**). (**D1**) Silencing of spastin results in stable MTs after Aβ treatment. Cells expressing shRNA (RFP-positive cells, dotted box, magnified in **D3**, arrows) show no MT reduction as neighbouring untransfected cells do (RFP-negative cells, solid box, magnified in **D4**, arrowheads). (**D2**) Silencing of spastin in control cells has no effect on microtubule density. (**D3**–**D5**) Magnification of boxed areas in (**D1**) and (**D2**).

©2013 European Molecular Biology Organization

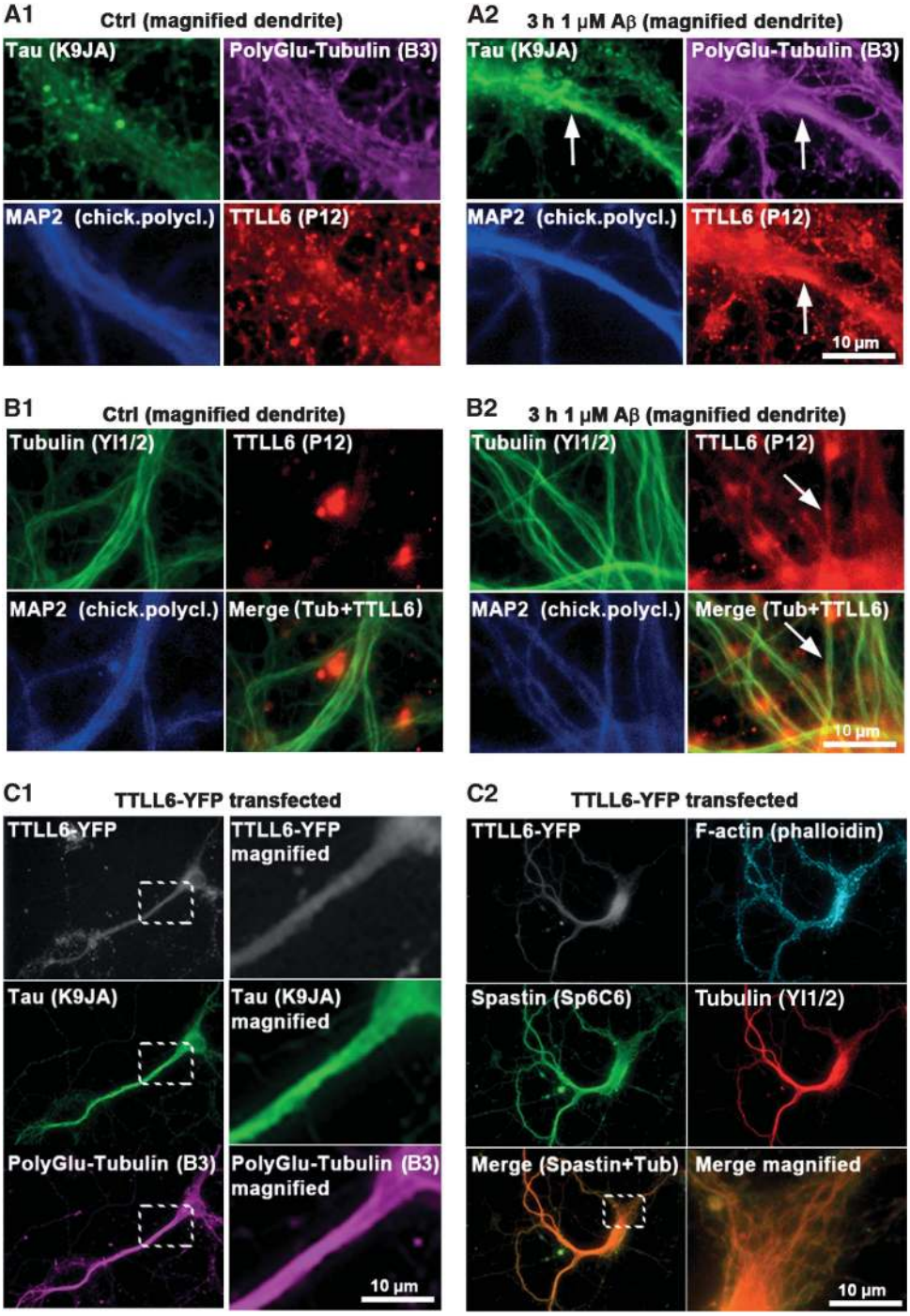

Figure 3 TTLL6 induces polyglutamylation of MTs and Tau missorting. (**A**, **B**) Primary rat hippocampal neurons 21DIV treated with 1 μM Aβ for 3 h. MAP2 was used as a marker for the somatodendritic compartment. (**A**) Increases in dendritic polyglutamylation of MTs correlate with dendritic appearance of TTLL6 and Tau missorting (note colocalization indicated by arrows in **A**2) after Aβ treatment. Only basal/background levels of polyglutamylation of MTs, and no presence of TTLL6 or Tau can be detected in controls (**A1**). (**B**) Fixation and extraction to preserve MTs indicate recruitment of TTLL6 to MTs after Aβ treatment (**B2**; arrows), no recruitment is apparent in the case of controls (**B1**). (**C**) YFP-tagged TTLL6 was transfected into primary neurons for 1 day. (**C1**) Transfection of TTLL6 results in increased polyglutamylation and missorting of Tau. Right panels show magnification of boxed areas. (**C2**) TTLL6-transfected cells show enhanced spastin recruitment to MTs; merged images of spastin and tubulin show colocalization (lower right panel shows magnification of boxed area in lower left panel).

was reduced, indicating less stable MTs (Figure 7G1, right panels and Figure 7G2 for quantification).

Next, we tested whether Tau and TTLL6 could be co-immunoprecipitated. TTLL6 could precipitate full-length hTau40 and the N-terminal half of Tau (construct K25, containing the proline-rich domain without the inserts; Gustke *et al*, 1994), but not the C-terminal half (construct K10; Figure 7H). Thus, the Tau–TTLL6 interaction is localized in the N-terminal half, and independent of the number of inserts, the repeat domain, and the C-terminal tail. Of note, transfection of wt-Tau, KXGE-Tau or KXGA-Tau all resulted in translocation of TTLL6 from the soma to the dendrites,

 ©2013 European Molecular Biology Organization

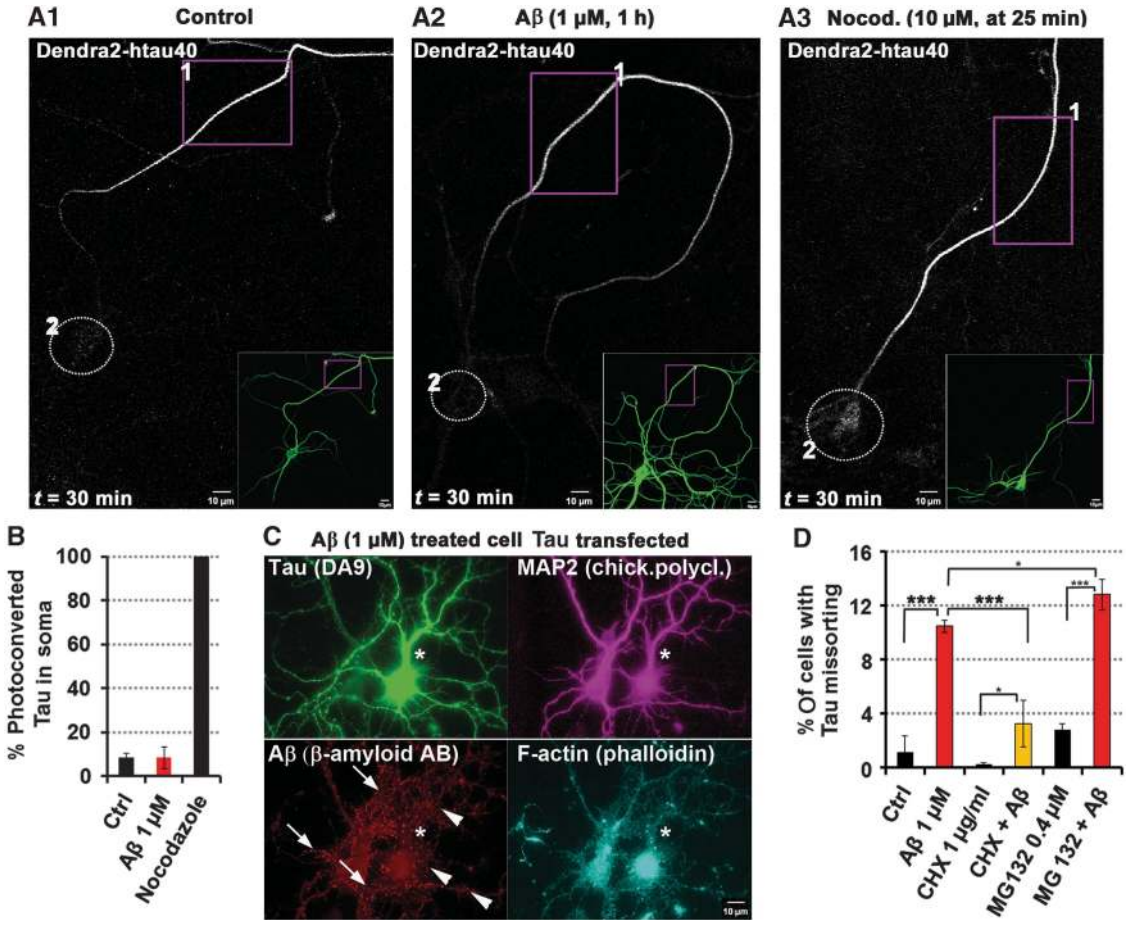

Figure 4 Missorted Tau is not axonally derived but newly synthesized. (**A–C**) Primary rat hippocampal neurons 23DIV were transfected with hTau40 fused to the photoconvertible FP Dendra2 (Tau^{D2}) 5 days prior to treatment/observation. (**A1**) Transfected Tau^{D2} displays homogeneous distribution in the cell (insert). After photoconversion in ROI 1 (box) at $t = 0$ min, Tau^{D2} propagation is restricted to the axon, Tau^{D2} does not reach the cell body (circle, ROI 2) even after 30 min of observation. (**A2**) Treatment with Aβ (1 μM, 1 h) prior to photoactivation does not change the Tau^{D2} propagation behaviour, Tau^{D2} propagation is still restricted to the axon, and does not reach the cell body (circle). (**A3**) Nocodazole treatment at $t = 25$ min induces rapid diffusion of Tau^{D2} across the Tau diffusion barrier; Tau reaches the cell body (circle). (**B**) Quantification of photoconverted Tau^{D2} fluorescence intensities in the cell body 30 min after photoactivation of conditions from (**A1**) to (**A3**). (**C**) After transfection with Tau^{D2}, imaging and treatment with Aβ (1 μM), cells were fixed and stained as indicated. In transfected cells (star), despite higher levels of Tau, Aβ is associated to dendrites (arrowheads, lower panel), comparable to cells with weak missorting of endogeneous Tau (arrows, lower panel) after Aβ treatment. Both the presence of spines and MAP2 indicate the somatodendritic compartment. (**D**) Quantification of missorting after treatment with Aβ (1 μM, 3 h) and modulators of protein homeostasis. Co-treatment with the translation inhibitor cycloheximide (1 μg/ml) reduces Tau missorting, whereas treatment or co-treatment with the proteasome inhibitor MG132 (0.4 μM) showed a trend to increase the amount of missorting.

independently of exposure to Aβ (e.g., Figure 7D). Hence, Tau missorting mediates TTLL6 mislocalization independently of phosphorylation in the repeat domain.

To clarify the role of Tau phosphorylation for Aβ toxicity, we transfected wild-type Tau in different phospho-variants, either pseudophosphorylated at the four KXGS motifs (KXGE-Tau) or KXGA-Tau (non-phosphorylatable). KXGE-Tau has only a weak affinity for MTs and diffuses rapidly, while KXGA-Tau binds tightly to MTs and diffuses slowly (Konzack *et al*, 2007). We observed that transfected KXGA-Tau moved into dendrites and spines, but did not re-sensitize TauKO cells to AβO (Figure 8). As in wild-type cells, AβOs were still targeted to the spines of transfected dendrites, but there was only moderate elevation of Ca^{++}, similar to untransfected TauKO neurons (~20%, see above and Supplementary Figure S11). There was also no additional loss of spines, TTLL6 moved into dendrites but MTs did not become polyglutamylated, spastin was not recruited, and MTs remained stable (Figure 8A and B; Supplementary Figure S11b–d).

In contrast to KXGA-Tau, KXGE-Tau (like wild type-Tau) did re-sensitize TauKO cells to AβO that induced pronounced spine loss, along with polyglutamylation of MTs, spastin recruitment, and MT decay (Figure 8A and B; Supplementary Figure S11). In fact, KXGE-Tau proved to be particularly detrimental to cells even without AβO treatment: mitochondria were clustered in cell bodies, and spine number and F-actin content in spines were reduced up to a complete loss of F-actin (Figure 8C). KXGE-Tau showed a pronounced localization to F-actin containing structures, notably in spines (Figure 8C1 and C2), whereas localization of wt-Tau to spines was negligible and KXGA-Tau moved into spines but had no apparent effect (Figure 8C3). This suggests that Tau phosphorylated in the repeat domain, at KXGS motifs, interacts with (not necessarily directly by binding) and impairs the actin cytoskeleton.

©2013 European Molecular Biology Organization

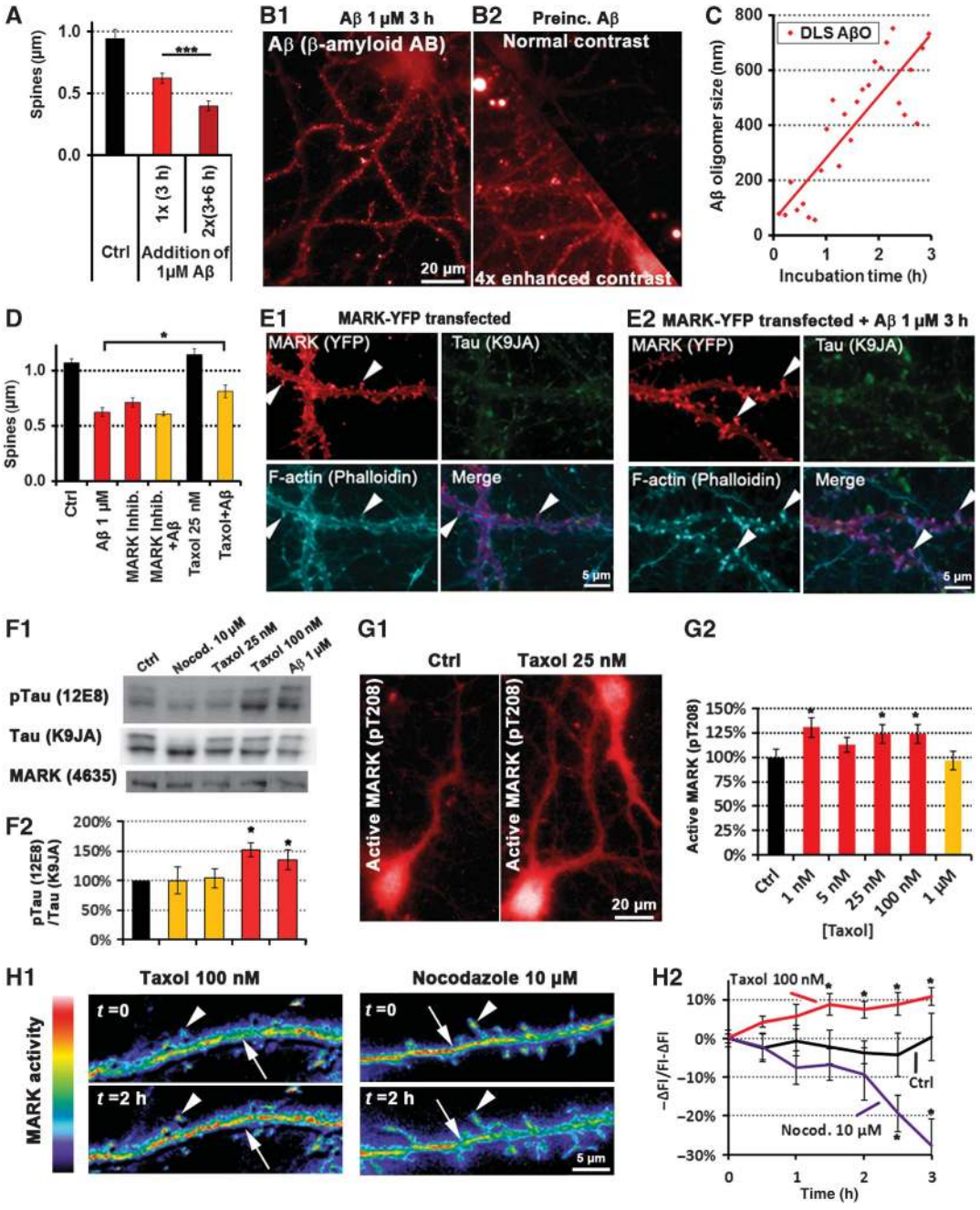

Figure 5 MARK re-establishes Tau polarity and restores spines after Aβ loses its toxicity. Primary rat hippocampal neurons (21DIV) were treated with 1 µM Aβ or as indicated. (**A**) Quantification of spine number in control conditions and after one insult or two sequential insults with a lag time of 3 h indicate that neurons do not become resistant; spine loss increases with the hit number. (**B**) Aβ targeting to neurons. (**B1**) Normally oligomerized Aβ targets neurons. (**B2**) AβO was pre-incubated for 3 h under cell-culture conditions at the usual concentration (1 µM), and then applied to cells for 3 h. Aβ targeting to dendrites becomes apparent only with enhanced contrast (lower half shows mirrored image of upper half, but contrast was enhanced four-fold). (**C**) Dynamic light scattering (DLS) of AβO at 37°C reveals that even at low concentrations (shown here: 1 µM) AβO rapidly grow in size. (**D**) Quantification of spine number with MARK modulators after 3 h exposure. The MARK inhibitor F7 (compound 39621; 1 µM, 3 h) decreases the number of spines similarly to Aβ, while taxol (25 nM) as an MARK activator protects spines from Aβ toxicity. (**E**) YFP-tagged MARK2 was transfected and expressed for 3 days. (**E1**) YFP-MARK2 localizes to the somatodendritic compartment and is enriched in spines (magnified images of dendrites). Arrowheads indicate spines. (**E2**) Transfected MARK2 protects against Aβ-induced missorting of Tau. Magnified images of dendrites; 3 days after transfection, cells were treated with 1 µM Aβ for 3 h and stained for total Tau. MARK2-transfected neurons (left panel) do not show missorting of Tau or spine loss (spines are indicated by arrowheads). (**F1**) Western blots with antibodies against pTau (12E8, phosphorylation at KXGS motifs) and total Tau and MARK shows increased phosphorylation only in the case of high taxol concentration (100 nM) and Aβ (1 µM), but not with nocodazole (10 µM) or low taxol concentration (25 nM) and no change in total Tau or MARK expression. (**F2**) Quantification of (**F1**). (**G**) Cells were treated for 3 h with different concentrations of taxol, and stained with an antibody recognizing MARK when phosphorylated at its activation site (pT208). (**G1**) 25 nM taxol results in increased immunofluorescence throughout the cell. (**G2**) Quantification of several concentrations of taxol reveals increase in MARK phosphorylation over a broad range of concentrations. (**H**) Cells were transfected with an FRET-based MARK activity reporter for 4 days, and treated with taxol (100 nM) or nocodazole (10 µM). (**H1**) Ratiometric imaging of the MARK activity reporter shows increased FRET 2 h after taxol addition (left panel) indicating increased MARK activity in spines (arrowhead) and the dendritic shaft (arrow). Two hours after nocodazole addition (right panels), MARK activity is decreased in spines (arrowhead) and the dendritic shaft (arrow). (**H2**) Quantification of time-lapse imaging.

 ©2013 European Molecular Biology Organization

Discussion

Cascade of Aβ-induced events leading to Tau missorting and MT loss

In the present study, we focussed on the link between AβO and the neuronal cytoskeleton, notably the phosphorylation/missorting of Tau and breakdown of MTs because these features are early hallmarks of AD (Braak and Braak, 1991; Spires-Jones *et al*, 2009). As an experimental approach, we chose mature hippocampal neurons in three forms: (i) wild-type, (ii) from TauKO mice, or (iii) from TauKO mice after re-introduction of Tau or Tau phospho-mutants. We observed the AβO-induced response of Tau and of related cytoskeletal structures, notably MTs and affiliated proteins.

The neuronal responses to AβOs can be divided into four stages (Figures 1F1, F2 and 2B; Supplementary Figure S4b): rapid (maximum at ∼1 h), medium (∼3 h), slow (6 h), and very slow (>12 h).

The rapid responses include the rise in intracellular Ca^{++}, loss of spines, and loss of MTs. The Ca^{++} response is actually slow compared to instantaneous effects of glutamate (Supplementary Figure S10), but in the case of AβO exposure it starts within minutes (Rui *et al*, 2006; Zempel and Mandelkow, 2012). This precedes MT breakdown (peaking at ∼1 h) and spine loss (∼1 h).

MT breakdown has the potential to destroy spines in at least two ways: MT-dependent traffic would slow down, for example, that of mitochondria (Thies and Mandelkow, 2007), and excursions of MTs into spines for delivery of regulatory proteins would cease (Jaworski *et al*, 2009). MT loss alone is enough to explain impaired mitochondrial distribution, but other factors, like Tau-mediated transport impairments or elevated Ca^{++}, might also contribute (see e.g., Ebneth *et al*, 1998 and Wang and Schwarz, 2009).

However, experiments with TauKO cells show that Ca^{++} alone is sufficient to cause spine decay, independently of MT breakdown (see below). Thus, Ca^{++} could exert spine damage by more than one mechanism, either via MTs or other pathways, for example, activation of calpain, induction of ROS, or local caspase-3-dependent spine apoptosis (Klein, 2006; Bano and Nicotera, 2007).

Given that both Tau missorting and MT loss are downstream of Aβ-induced Ca^{++} elevation, the question arises how these two features are related. In principle, Tau can stabilize MTs and is therefore not likely to cause MT decay. On the other hand, cellular MTs are highly sensitive to Ca^{++} in the low μM range (1–4 μM). A direct induction of MT depolymerization by Ca^{++} can be ruled out, as intracellular $[Ca^{++}]$ does not exceed 0.5 μM. This increase in Ca^{++} through NMDA receptors is sufficient to trigger effectors, for example, calcineurin (Shankar *et al*, 2007), but does not reach the levels required for direct MT breakdown (Schliwa *et al*, 1981).

A medium response time to AβOs and Ca^{++} is observed for the buildup of missorted Tau in dendrites. Total Tau becomes already prominent concomitant with MT breakdown (1 h) but continues to rise up to 3 h. An interpretation is that breakdown of MTs allows diffusion of Tau between cell compartments, not restricted by attachment to MTs (Konzack *et al*, 2007; Li *et al*, 2011). By contrast, phospho-Tau (antibody 12E8) follows with some delay (peak at ∼5–6 h), roughly parallel to the activation of MARK (see below).

The rapid disappearance of MTs in dendrites is one of the unexpected enigmas among the Aβ-induced responses (King *et al*, 2006). When considering possible causes, several mechanisms come to mind:

(i) Withdrawal of MAPs, resulting in lower MT stability: this is unlikely because the level of MAPs actually increases due to the influx of Tau.
(ii) Sensitivity to Ca^{++}: also an unlikely explanation because MTs do not break down in TauKO cells and because exposing TauKO cells to high Ca^{++} does not decrease MT stability (Figure 6C5).
(iii) Active cleavage by MT-severing proteins: this is compatible with the observations. In fact, spastin had a clear response in AβO-treated cells, and knockdown of spastin by shRNA prevented MT disruption after AβO exposure (Figure 2). This is consistent with spastin's widespread distribution in neurons and its role in branch formation (Riano *et al*, 2009; Ye *et al*, 2011). Given the potency of severing enzymes in remodelling the cytoskeleton, their activity must be kept under tight control.

For spastin, this is achieved by local post-translational modifications of MTs, notably polyglutamylation of near-C-terminal Glu residues which serves as a signal for spastin recruitment. The modification is in turn achieved by enzymes of the TTLL family, in particular TTLL6 in neurons (Janke and Kneussel, 2010; Lacroix *et al*, 2010). Indeed, while TTLL6 is normally mainly in cell bodies, it moves into affected dendrites after AβO exposure or after Tau overexpression (Figures 3 and 7). It is also conceivable that Tau forms a ternary complex with tubulin and spastin, but as the affinity of Tau to tubulin dimers compared to MTs is low, and TTLL6 activity triggers MT breakdown, a ternary complex seems unlikely.

It should be noted that katanin can also be activated by polyglutamylation of MTs (Lacroix *et al*, 2010). However, katanin is downregulated during maturation and is present mainly in neuritic tips of developing processes (Yu *et al*, 2005), is inactivated by Ca^{++} (Iwaya *et al*, 2012), and Tau has been shown to block MT-severing mediated by katanin, but not spastin (Qiang *et al*, 2006; Sudo and Baas, 2010). Because of low levels of katanin in dendritic shafts and adult neurons, and the presence of both elevated Ca^{++} and Tau in Tau-missorted neurons, katanin is unlikely to play a major role in our paradigm. Indeed, there was no change in distribution or levels of katanin-p80 or katanin-p60, and silencing of katanin did not prevent Tau missorting or MT loss (Supplementary Figure S5).

From these observations, a chain of events from Aβ to MT breakdown can be proposed (Figure 8D):

AβOs on spines → rise of Ca^{++}/loss of spines → dendritic missorting of Tau → transport of TTLL6 into dendrites → polyGlu modification of MTs → spastin recruitment → severing of MTs.

Non-axonal origin of missorted Tau

Given the importance of somatodendritic Tau missorting as an early marker of AD, one obvious question is: where does the missorted Tau come from? In mature neurons, Tau is largely axonal (Binder *et al*, 1986). Consistent with this, the earliest signs of pathological Tau phosphorylation occur in axons (Braak and Del Tredici, 2011; Braak stage '0'), followed

©2013 European Molecular Biology Organization

by phosphorylation and later aggregation in cell bodies and dendrites. The basis for axonal Tau sorting in mature neurons is still not well understood, and several protein-based or mRNA-based mechanisms may work in parallel (Kanai and Hirokawa, 1995; Aronov *et al*, 2001; Nakata *et al*, 2011), including a retrograde barrier for Tau at the AIS (Li *et al*, 2011). Probing the barrier after AβO exposure showed that it remained tight. This agrees well with the fact that axonal Tau is in a low state of phosphorylation in mature axons, and the level of axonal MARK2 is low as well. Also, we did not observe axonal MT loss, polyglutamylation, or spastin recruitment, indicating that axonal Tau would remain bound to MTs and retained in the axon. In fact, basal polyglutamylation is higher in axons than in dendrites

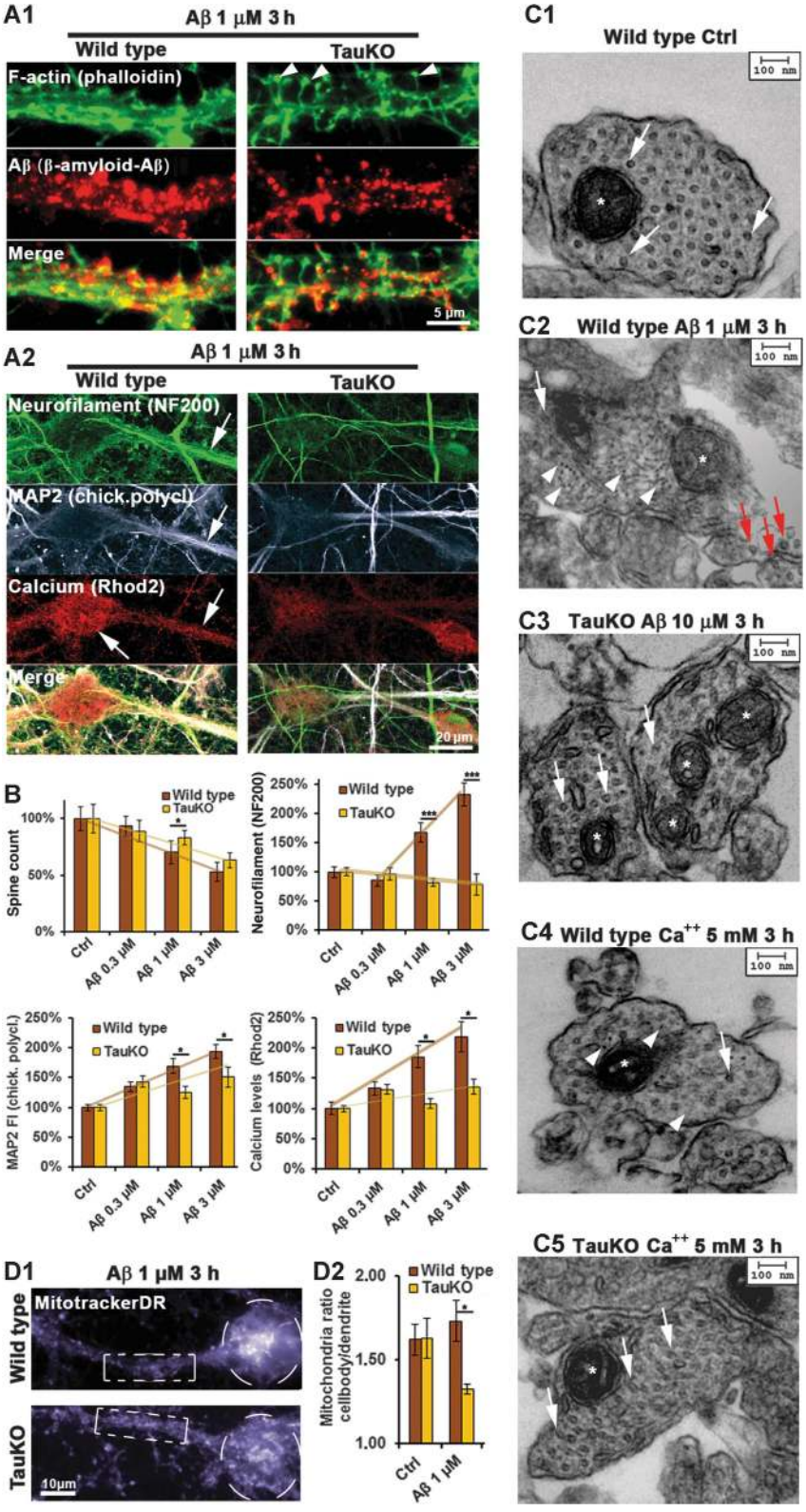

©2013 European Molecular Biology Organization

(Janke and Kneussel, 2010), possibly aiding Tau retention (Tau has a net positive charge, while polyglutamylation is negatively charged). Thus, axonal Tau is not likely to contribute to the buildup of dendritically missorted Tau. The alternative explanation is that part of the newly synthesized Tau in the cell body is no longer routed into the axon, but becomes free to enter the dendrites. This is indeed the case, since blockage of both global and Tau protein synthesis strongly reduces dendritic missorting of Tau after AβO exposure.

Reversibility of Aβ toxicity

A remarkable feature of the slow and very slow response to AβOs is the gradual return of the abnormal changes to near-baseline levels, beginning at ∼6 h (Figures 1F and 2B; Supplementary Figure S4b). The onset of recovery coincides roughly with the structural rearrangements in the AβOs towards larger species where the toxic potential is lost (Figure 5; Kuperstein *et al*, 2010; Bieschke *et al*, 2012). This emphasizes that Aβ-induced cell damage can be repaired once the toxic stimulus disappears; once recovered, cells remained healthy.

The recovery process is accompanied by a transient rise in active MARK that peaks at 6 h (Figure 1F). This kinase is important because its phosphorylation sites on Tau appear very early in AD and in mouse models. Other sites of Tau are also phosphorylated in response to Aβ (Zempel *et al*, 2010), but MARK disrupts Tau–MT interactions and is enriched in neurons (Drewes *et al*, 1997; Augustinack *et al*, 2002; Thies and Mandelkow, 2007). In differentiating neurons, it is active in growth cones (Timm *et al*, 2011), but later in dendrites, particularly spines (Hayashi *et al*, 2011). The activation of MARK appears to be part of the recovery, consistent with the observation that transfection of neurons with MARK2 makes them resistant against the AβO challenge (i.e., no loss of spines or MTs, no missorting of Tau). The transfected MARK2 localizes mainly to spines and evidently bolsters their defense against AβOs (Figure 5). This could be due to the ability of MARK to stabilize F-actin (Matenia *et al*, 2005) and maintain mature spines by enabling transient MT invasion (Hayashi *et al*, 2011). Of note, the MT-stabilizer taxol prevents spastin induced breakdown of MTs (Salinas *et al*, 2005), and prevents MT loss and Tau missorting after Aβ exposure (Zempel *et al*, 2010). Taxol also prevented loss of spines and activates MARK over a broad range of concentrations, while the MT-destabilizer nocodazole inactivates MARK (Figure 5F–H); thus, stable MTs induce MARK activity. MARK activity in turn is essential for spine protection and maintenance, but not for Tau polarity: specific inhibition did not induce Tau missorting within the timeframe investigated here (Supplementary Figure S9). Overall, the net result of taxol treatment is that MTs are not disrupted, Tau is not missorted, MARK is activated, and spine loss is reduced (Figure 5).

Absence of Tau protects against AβO by preventing spastin-mediated MT severing

Aβ-based models with varying levels of Tau provided evidence for Tau as a mediator of Aβ toxicity (Rapoport *et al*, 2002; Roberson *et al*, 2007; Ittner *et al*, 2010), but also as a protective agent in aged animals (Dawson *et al*, 2010; Lei *et al*, 2012). This prompted us to study the Aβ-Tau cascade in neurons from TauKO mice (Dawson *et al*, 2001). The major outcome was that TauKO neurons showed dramatically reduced levels of toxicity: AβOs still bound to spines, but there was little loss of spines, weak Ca^{++} elevation, TTLL6 was not recruited to MTs, no polyglutamylation of MTs, no spastin recruitment, no MT breakdown, no impairment of mitochondria distribution, and no missorting of neurofilaments. Thus, Tau is responsible for the toxic consequences of AβOs. Several scenarios are conceivable:

(i) A minor fraction of Tau, not visible by our methods, might be present in the spines of wild-type cells and could facilitate Ca^{++} influx after following AβO exposure, leading to loss of spines and MTs. This would be consistent with the proposal that AβO interacts with NMDAR or other receptors (Klein, 2006; Shankar *et al*, 2007; Lauren *et al*, 2009), and with the idea that a small fraction of Tau might facilitate dendritic localization of signalling molecules such as fyn (Ittner *et al*, 2010).

(ii) Although missorted Tau peaks only in stage 2 after ∼3 h (Figure 1F1), the initial half invades dendrites rapidly in stage 1 after AβO exposure, coincident with loss of MTs and spines. This fraction of Tau can invade spines, could disrupt their functions, and perhaps facilitate accumulation of TTLL6 and spastin recruitment. It is known that Tau can bind to F-actin networks, membrane-associated proteins (e.g., annexins), various proteins with SH3 domains, chaperones (e.g., Hsc70), and other proteins whose functions might be perturbed (Sarkar *et al*, 2008; Whiteman *et al*, 2009) and thus cause the toxicity of AβO.

Figure 6 Tau deficiency does not protect against Aβ association to dendrites and transient spine loss, but protects against loss of MTs, neurofilament invasion, and loss of mitochondria. Primary wild-type (wt) and TauKO hippocampal neurons aged 19–20DIV. (**A1**) Three hours after exposure to Aβ, Aβ staining shows solid association with dendrites of both wt and TauKO cells (middle panels). Dendritic spine number (upper panels) is reduced in both cases, arrowheads indicate remaining spines in the case of TauKO neurons (right panels). (**A2**) Left panels: treatment of wt cells results in strong somatodendritic missorting of neurofilaments and increase in Ca^{++} and MAP2 (arrows). Right panels: treatment of TauKO cells with Aβ does not result in missorting of neurofilaments. MAP2 and Ca^{++} are only slightly elevated. (**B**) Quantifications of (**A1**) and (**A2**). Upper left panel: quantification of (**A1**) reveals a trend to more stable spines in the case of TauKO cells. Upper right panel: only wt cells show neurofilament invasion. Lower panels: wt cells show a dose-dependent increase in dendritic MAP2 and Ca^{++} levels, while there is only a slight increase in TauKO cells. (**C**) Electron microscopy of thin cross-sections of wt and TauKO hippocampal dendrites of cells treated with AβO or Ca^{++} as indicated. Stars indicate mitochondria. (**C1**) Control dendrites show a dense packing of MTs (arrows) and no neurofilaments. (**C2**, **C4**) Wt dendrites show loss of MTs in the dendrites (indicated by arrows), but not in axons (red arrows, c2), and neurofilament invasion (arrowheads). (**C3**, **C5**) TauKO neurons do not show MT loss after exposure to Aβ or Ca^{++} and no neurofilament invasion. (**D**) Cells were treated with Aβ for 3 h and stained for mitochondria. (**D1**) After exposure to Aβ, in wt cells (upper panel) mitochondria are cluster in the cell body (circle) and are lost in the dendrite (box), while in TauKO cells (lower panel) mitochondria density is similar in the cell body (circle) and the dendrite (box). (**D2**) Quantification of the ratio of mitochondria staining in the soma versus dendrite reveals clustering of mitochondria in the cell body in the case of wt neurons, whereas in TauKO neurons mitochondria are reduced in the soma and elevated in the dendrite.

©2013 European Molecular Biology Organization

(iii) Activation of synaptic receptors by AβOs causes rapid changes in electrical activity (Snyder *et al*, 2005; Kuperstein *et al*, 2010). This could affect the neuronal cell culture as a whole with far reaching consequences, including Tau-dependent network activities (Palop and Mucke, 2009).

To confirm Tau's role in Aβ toxicity, the largest isoform was re-introduced into TauKO neurons. This indeed re-establishes all aspects of AβO toxicity, that is, Ca^{++} rise, loss of spines, polyglutamylation, severing of MTs by spastin, and impaired distribution of mitochondria. The Tau-KXGE mutant, designed for (pseudo-) phosphorylation and low MT affinity, is also toxic, even more than wild-type Tau. By contrast, the Tau-KXGA mutant, which retains a high affinity for MTs, does not re-introduce toxicity (Figure 8; Supplementary Figure S11). In all cases, translocation of TTLL6 into dendrites is enhanced, in line with interaction of TTLL6 with the N-terminal half of Tau, which is unaffected in these pseudophosphorylation mutants of Tau (Figure 7H). But polyglutamylation, spastin recruitment, and MT decay take place only in the case of wild-type Tau and KXGE-Tau. Thus, the repeat domain of Tau must be phosphorylatable for re-sensitizing neurons to AβO toxicity. Since phosphorylation at KXGS motifs detaches Tau from MTs (Drewes *et al*, 1997), this suggests a non-MT function of Tau that could become toxic. Several interactions become prominent when Tau loses its MT affinity, either by phosphorylation (as in the present case), or by truncation and other modifications (Mandelkow and Mandelkow, 2012). Regarding spine function and stability, three types of non-MT interactions are notable:

(i) Tau phosphorylated at KXGS sites can become missorted and enter spines, cause their decay, could bind to and disrupt the actin cytoskeleton (Figure 8C) (Fulga *et al*, 2007; Sharma *et al*, 2007; Thies and Mandelkow, 2007;

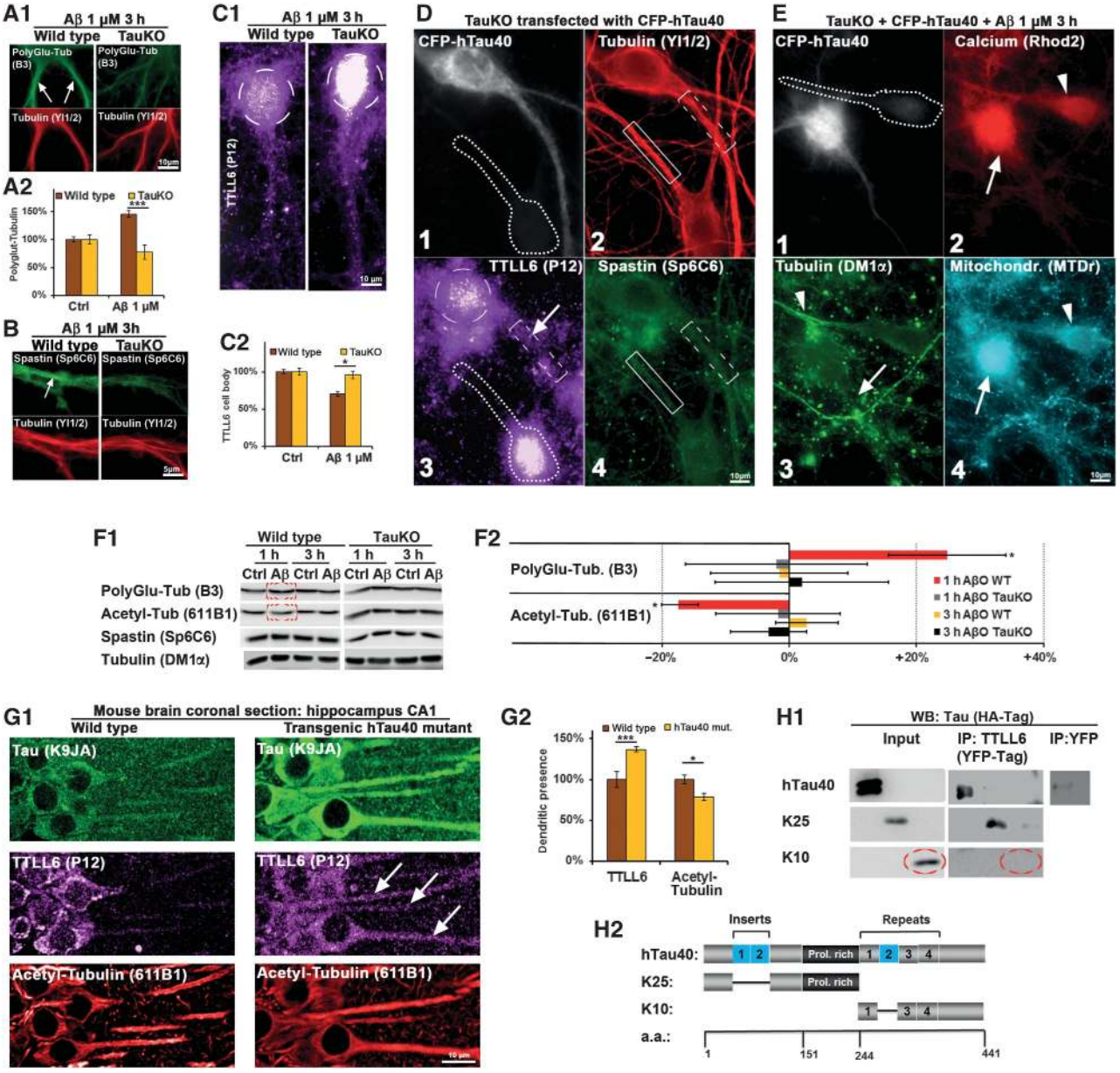

©2013 European Molecular Biology Organization

Hoover *et al*, 2010; Morris *et al*, 2011). Actin can then leave spines and co-aggregate in the dendritic shafts with p-Tau and cofilin as 'actin rods' (Bamburg and Bloom, 2009; Whiteman *et al*, 2009).

(ii) The proline-rich domain of Tau contains PXXP motifs able to bind SH3-domain proteins, including several signalling kinases (e.g., fyn, lck, src, PI3K; Williamson *et al*, 2008), and it has been proposed that Tau can cause misregulation of NMDA receptors via fyn (Ittner *et al*, 2010).

(iii) Tau can interact with nucleic acids. This may play a physiological role (e.g., protection against stress; Sultan *et al*, 2011), but missorted Tau could also interfere with local mRNA translation at spines. In the context of AD, it is notable that the Tau–RNA interaction can trigger pathological aggregation (Kampers *et al*, 1996).

Remarkable features in our observations are the two seemingly antagonistic roles of MARK: active MARK in spines protects against AβO insults and promotes recovery, whereas phosphorylation of Tau by MARK makes Tau toxic and causes spine decay. The resolution of this discrepancy probably lies in the distinct spatio-temporal activation of MARK versus Tau, that is, MARK is active in healthy spines where Tau is absent, while Tau-induced toxicity arises only after it becomes missorted and phosphorylated.

Acute treatment with AβO of primary neurons, despite the high maturation state used in this study, is very different to the extremely slow disease progression in AD, which takes place over decades. Still, Aβ levels are fluctuating depending on brain region, activity, and stress (Kang *et al*, 2009; Wei *et al*, 2010; Bero *et al*, 2011). Thus, constant fluctuation requires a dynamic adaptation or reversibility, which we describe here. As TTLL6 mislocalization, polyglutamylation, and spastin recruitment are Tau dependent, Aβ depositing mice likely will not show this phenotype, because Tau pathology is minor in mice that are not transgenic for Tau. In Tau tg mice, mislocalization of TTLL6 and reduced dendritic MT stability could be readily observed (Figure 7G1 and G2). This is in line with experiments demonstrating decreased MT stability and cognitive deficits in Tau tg mice, both of which can be prevented by taxol (Ishihara *et al*, 1999).

With regard to therapeutic approaches, our results suggest that Aβ-induced toxicity can be intercepted at several levels: lowering the tonic increase in dendritic Ca^{++}, prevention of Tau missorting and/or reducing its phosphorylation in the repeat domain, stabilization of dendritic MTs (by drugs (not proteins) that stabilize MTs such as taxotere, prevention of polyglutamylation and/or local inactivation of spastin). Indeed, epothilone D (an analogue of taxotere) has already been shown to be beneficial in Tau transgenic mice (Zhang *et al*, 2012). Mild loss-of-function mutations of spastin also should prevent MT defects and possibly cognitive decline in Tauopathies, but this correlation has not been explored. Future experiments will show which of these pathways is most relevant for MT stability and which is most promising for therapeutic approaches.

Materials and methods

Microscopy

Light and electron microscopy set-ups, live-imaging conditions, photoconversion, and quantification procedures were described previously (Zempel *et al*, 2010; Li *et al*, 2011). Additionally, a MetaMorph-based Leica DMI6000B equipped with incubator, heating and CO_2 incubator (all Leica provided (Pecon)) was used. For spontaneous Ca^{++} oscillations, primary neurons were plated at high density, aged for ~20DIV, labelled with Fluo4 or Fura2 (Invitrogen), and time-lapse movies were recorded of at least three different fields for 2 min each. MARK-activity reporter was

Figure 7 Tau deficiency prevents AβO-induced polyglutamylation, spastin recruitment, and TTLL6 transport into dendrites. Transfection of human Tau causes TTLL6 transport into dendrites and re-establishes AβO toxicity in TauKO cells. (**A–C**) Primary wt and TauKO hippocampal neurons aged 19–20DIV were treated with Aβ (1 μM, 3 h) and stained as indicated. (**A1**) In wt cells (left panels), Aβ treatment results in increased dendritic polyglutamylation (arrows). In TauKO cells (right panels), polyglutamylation of MTs remains at baseline levels after Aβ exposure. (**A2**) Quantification of (**A1**). (**B**) After Aβ exposure, spastin is recruited to MTs in the case of wt cells (left panels, arrow), but not in TauKO cells (right panels). (**C1**) After Aβ exposure, TTLL6 is reduced in the soma (circle) in the case of wt cells (left panel) compared to TauKO neurons (right panel). (**C2**) Quantification of TTLL6 levels in the cell body shows reduction in TTLL6 of wt cells. (**D**) Transfection of CFP-hTau40 results in translocation of TTLL6 from the soma into the dendrite, but no spastin recruitment and no loss of MTs. (1) CFP signal indicates transfected cell, neigbouring cell (dotted line) is not transfected. (2) Transfection of Tau does not change MT density (boxes indicate dendritic segments; transfected cell: dotted box; untransfected cell: solid box). (3) Tau-transfected cell shows translocation of TTLL6 into the dendrite (boxed; arrow); also note the reduction in the cell body (circle), while in the untransfected cell (dotted line) TTLL6 remains in the cell body. (4) Staining of spastin; Tau transfection does not change spastin recruitment. (**E**) Presence of Tau and AβO insult are necessary for MT loss, Ca^{++} rise, and clustering of mitochondria. TauKO cells were transfected with CFP-hTau40 for 3 days and then treated with Aβ 1 μM for 3 h. (1) TauKO cell transfected with CFP-hTau40 shows the CFP signal, neighbouring untransfected cell is indicated by dotted line. (2) Tau-transfected cell (arrow) shows strong Ca^{++} increase compared to untransfected cell (arrowhead). (3) Tau-transfected cell shows MT loss (arrow), while neighbouring cell displays normal MT density (arrowhead). (4) Tau-transfected cells show mitochondria clustering in the cell body (arrow) compared to untransfected cell (arrowhead). (**F1**) Western blot analysis of primary neurons shows an increase in polyglutamylation of microtubules, and a decrease in acetylation of microtubules only in wild-type neurons after 1 h of Aβ treatment, but no change after 3 h and no change in TauKO neurons, and no change in spastin or tubulin levels. The same membranes were used for polyglutamylation and acetylation of microtubules. (**F2**) Quantification of (**F1**). (**G**) Coronal sections of the CA1 region of the hippocampus of wild-type mice (left panels) and transgenic mice expressing human Tau (right panels) were stained for Tau with an antibody that detect both mouse and human Tau, TTLL6 and acetylated tubulin as a marker for stable microtubules. (**G1**) Upper panels: compared to wild-type mice, transgenic mice express more Tau; Tau is also strongly missorted into the somatodendritic compartment. Middle panels: in wild-type mice, TTLL6 is present mainly in the cell body, in transgenic mice it is also sorted into the dendrites (arrows). Lower panels: transgenic mice show lower levels of acetylated microtubules. (**G2**) Quantification of (**G1**). (**H**) HEK293 cells were transfected with HA-tagged versions of the longest human Tau isoform (hTau40), or the N-terminal half lacking both inserts (K25), or the C-terminal half without the second repeat (K10), plus TTLL6-YFP or YFP alone. (**H1**) Immunoprecipitation with an antibody against YFP pulled down hTau40 and K25, but not K10 in the case of TTLL-YFP transfection, while YFP alone did not pull down hTau40. Western blotting was done with an antibody against HA-Tag. (**H2**) Constructs used for the IP reveal that the presence of the C-terminal half, including the repeat domain, and both inserts in the N-terminal half are not required for binding of TTLL6 to Tau.

©2013 European Molecular Biology Organization

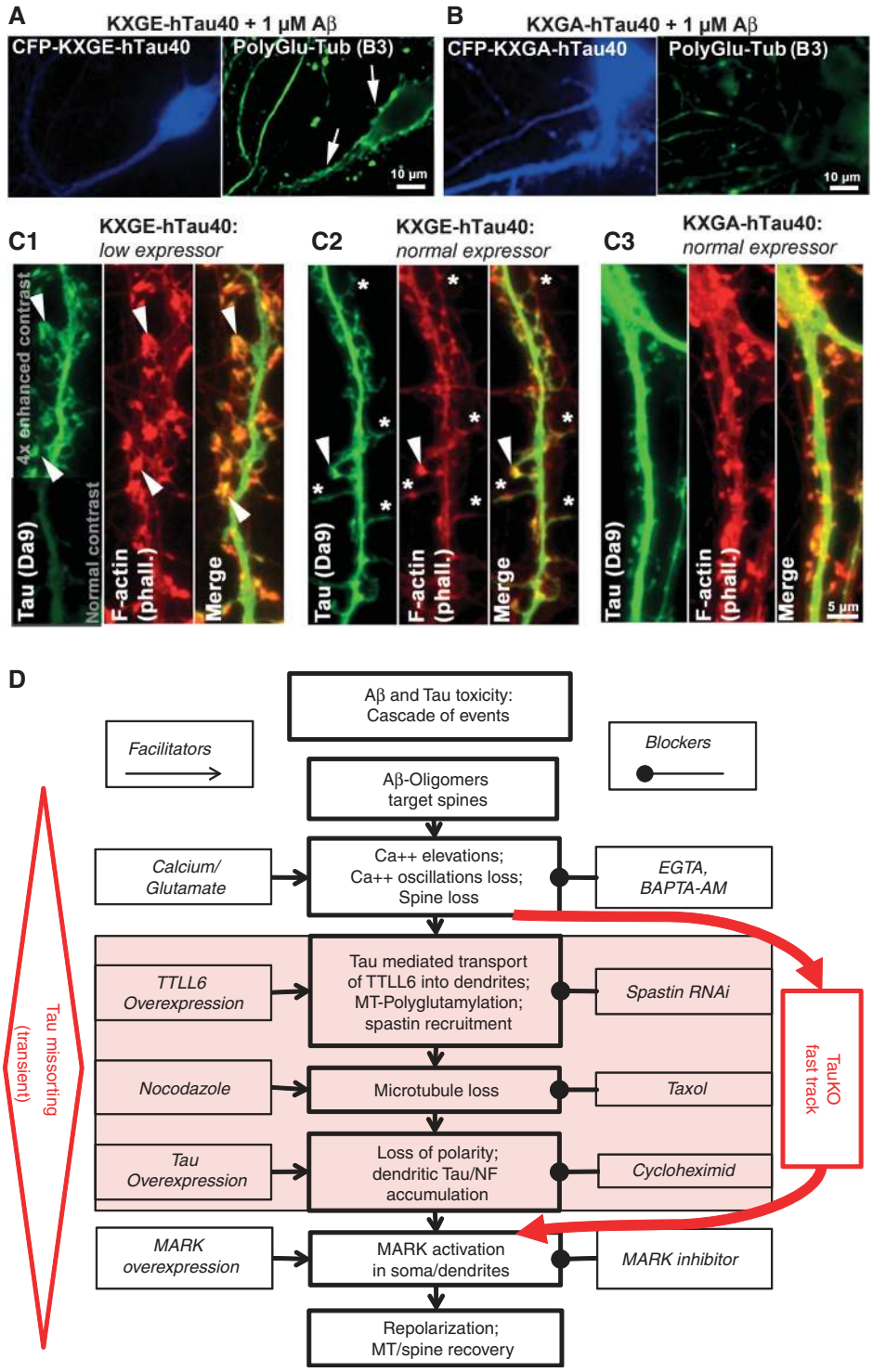

Figure 8 Re-introduction of CFP-hTau40 into TauKO neurons re-establishes Aβ-dependent toxicity when Tau is phosphorylatable or pseudo-phosphorylated at the KXGS motifs. Primary hippocampal neurons from TauKO mice were transfected for 3 days with CFP-tagged human Tau (hTau40) mutated at the KXGS motifs, either to KXGE (mimicking phosphorylation), or to KXGA (preventing phosphorylation) and treated with AβO for 3 h. (**A**) KXGE-Tau re-establishes Aβ-induced polyglutamylation of MTs. (**B**) KXGA-Tau does not permit enhanced polyglutamylation after exposure to Aβ. (**C**) TauKO primary hippocampal neurons were transfected with KXGE-Tau or KXGA-Tau, stained with antibody DA9 for signal enhancement. (**C1**) KXGE-Tau in low expression levels is enriched at F-actin containing spines (arrowheads). (**C2**) In normal expression levels, KXGE-Tau leads to depletion of F-actin in spines resulting in filopodia-like spines (stars), remaining F-actin containing spines are highly enriched with KXGE-Tau (arrowhead). (**C3**) KXGA-Tau is not enriched in spines and does not disturb F-actin. (**D**) Cascade of events leading from Aβ-induced damage (loss of Tau polarity, MTs and spines) to regeneration. The boxes in the center indicate the cascade of events after exposure to A?Os, boxes on the left indicate activators operating at different stages, boxes on the right indicate inhibitors. The shaded boxes indicate steps that are bypassed in the absence of tau, implying that missorting of cytoskeletal elements (e.g. NF) or breakdown of microtubules are largely circumvented.

©2013 European Molecular Biology Organization

imaged via ratiometric imaging and processing by the MetaMorph software (see also Timm *et al*, 2011).

Cell culture and transfection

Cells were cultured as described previously (Zempel *et al*, 2010), with slight modifications: AraC was added to rat cultures 3 days after plating, in a concentration of 0.5 μM, and to mouse cultures 4 days after plating in a concentration of 0.3 μM. Rat cultures were used after 3–4 weeks, mouse cultures after 19–21DIV. Adenoviral transfections were conducted as described (Thies and Mandelkow, 2007). Lipofectamine transfections were conducted as recommended by the manufacturer, but omitting OPTI-MEM since this does not allow culturing of mature neurons. Spastin RNAis were taken from Riano *et al* (2009), Tau RNAi sequence was taken from Sapir *et al* (2008), and katanin-p80 RNAi was taken from Sudo and Maru (2007). Katanin-p60 RNAi sequences were GAGUAAGGGCAGAGAGGAA and GAGAAGAACUGUUAAGAAU. All RNAi sequences were cloned into a pShuttle-mRFP/mTFP or pSuper vector. TTLL6-tGFP was obtained from Origene and recloned to TTLL6-YFP.

Immunostainings

Stainings were conducted by fixing cells overnight at 4°C with 3.7% formaldehyde (FA) in PBS and subsequent permeabilization for 5 min with 0.5% Triton-X in 5% BSA, followed by antibody incubations without further blocking. MT-based stainings were conducted by fixing the cells for 1 h at RT in 3.7% FA, 0.5% glutaraldehyde (GA), and subsequent permeabilization/extraction for 30 min with 0.5% Triton X-100 in 5% BSA, followed by antibody incubations without further blocking reagents or detergents (for antibody dilutions, see Supplementary Table S1). For mouse brain stainings, brains of 3–4 transgenic and control animals (Van der Jeugd *et al*, 2012) aged 8–9 months were fixed for 4 days at 4°C with 3.7% FA in PBS and 50 μm sections were cut with a Leica VT1200 vibratome. For quantification and statistical procedures, refer to Zempel *et al* (2010) and see below.

Quantification of compartment-specific fluorescence intensities

Dendrites were identified by a combination of positive MAP2 immunostaining, the presence of spines, typical branching pattern (60° in dendrites versus 90° in axons), lengths (<300 μm), width (>3 μm), and shape (constant decrease in diameter). Then, 20–30 μm of the proximal dendritic segment (distance from cell body ~30 μm for rat neurons, ~20 μm for mouse neurons) was selected as a region of interest (ROI) and the fluorescence intensities of co-stainings (e.g., Tau, stained with DA9, a mouse monoclonal antibody against aa 100–130, a kind gift of P Davies (NY, Albert-Einstein-College of Medicine); see also Supplementary Table S1 for other antibodies or labelling reagents and dilutions) were measured within the ROI. The same procedure was applied for control cells and treated cells. All quantifications, if not indicated otherwise, show ~30 cells on average per treatment. This method allows the unbiased evaluation of dendritic changes independently of a pre-selection on the basis of Tau distribution, and can be applied even to Tau KO neurons. Ca^{++} concentrations were estimated based on LaFerla (2002). Error bars represent s.e.m. from 3 to 4 independent experiments and cultures, or from 10 to 30 cells of a representative experiment. All experiments were conducted at least three times. Statistical analysis was done by Student's *t*-test or one-way ANOVA with *post hoc* Bonferroni for multiple comparisons with *, **, and *** indicating $P<0.05$, $P<0.01$, and $P<0.001$, respectively, versus control treatments as indicated.

AβO preparations

Aβ was completely dissolved in HFIP (Sigma) to 1 mM, aliquots were taken, and the HFIP was completely evaporated overnight in a Speedvac, and stored at −80°C. Directly before use, dried Aβ was dissolved in 40 mM NaOH to a 2-mM solution, and then immediately further diluted to a 100-μM solution in PBS (PAA). For the 7:3 mixture (Aβ40:Aβ42, see Kuperstein *et al*, 2010), the 100-μM solution was mixed at this point. For the preparation of the modified Aβ-derived diffusible ligands (mADDLs), DMSO was added at this point to constitute 2% of the final solution. Synthetic Aβ dimers, a kind gift of D Walsh (University College Dublin), were used as provided (58.5 μM stock, in 50 mM NH_4Cl). Solutions were incubated for 1 h at 37°C, or for initial characterization, left on ice for 1 h (see Supplementary Material). The Aβ mixture of Aβ40:Aβ42 = 7:3 was most potent in terms of spine loss and Tau missorting (see Supplementary Figure S2) and was therefore used for this study.

Other reagents/procedures

Aβ was from 21st Century Peptide, and other reagents were from SIGMA. ATP and LDH measurements and western blots are described in Zempel *et al* (2010). DLS measurements were conducted on a NanozetasizerS (Malvern Instruments) following the manufacturer's recommendations and AβO (7:3 mixture, see above) diluted in PBS to 1 μM. Immunoprecipitation was conducted using magnetic beads (Pierce) as recommended by the manufacturer. TTLL6-YFP and HA-tagged Tau or Tau fragments were expressed in HEK293 cells using calcium phosphate transfection. IP buffer was 50 mM NaCl, 50 mM Tris–HCl (pH 6.8), 5 mM $CaCl_2$, 0.05% Triton-X, 0.001% PMSF, and protease inhibitor mix (LaRoche).

Supplementary data

Supplementary data are available at *The EMBO Journal* Online (http://www.embojournal.org).

Acknowledgements

We thank Yvonne Biederbick and Annika Bülow for help with primary cultures, Sabrina Hübschmann for help with cloning, Peter Davies (Albert Einstein College, NY) for Tau antibody DA-9, Peter Seubert (Elan, South San Francisco, CA) for Tau antibody 12E8, David Sharp (Albert Einstein College, NY) for katanin antibody, Dominic Walsh (Harvard Univ., Boston, MA) for synthetic Aβ dimers. This research was supported by DZNE, MPG, Wellcome Trust/MRC, EU-FP7 (Memosad), Tau Consortium.

Author contributions: HZ and E-MM designed the study; HZ and JL performed the experiments, YK and HZ conducted the photoconversion experiments; JB supplied plasmids and adenoviruses; HZ, E-MM and EM analysed the data and wrote the paper; HD provided the TauKO mouse line.

Conflict of interest

The authors declare that they have no conflict of interest.

References

Aronov S, Aranda G, Behar L, Ginzburg I (2001) Axonal tau mRNA localization coincides with tau protein in living neuronal cells and depends on axonal targeting signal. *J Neurosci* **21:** 6577–6587

Augustinack JC, Schneider A, Mandelkow EM, Hyman BT (2002) Specific tau phosphorylation sites correlate with severity of neuronal cytopathology in Alzheimer's disease. *Acta Neuropath* **103:** 26–35

Baas PW, Karabay A, Qiang L (2005) Microtubules cut and run. *Trends Cell Biol* **15:** 518–524

Bamburg JR, Bloom GS (2009) Cytoskeletal pathologies of Alzheimer disease. *Cell Motil Cytoskeleton* **66:** 635–649

Bano D, Nicotera P (2007) Ca2+ signals and neuronal death in brain ischemia. *Stroke* **38:** 674–676

Bero AW, Yan P, Roh JH, Cirrito JR, Stewart FR, Raichle ME, Lee JM, Holtzman DM (2011) Neuronal activity regulates the regional vulnerability to amyloid-beta deposition. *Nat Neurosci* **14:** 750–756

Bieschke J, Herbst M, Wiglenda T, Friedrich RP, Boeddrich A, Schiele F, Kleckers D, Lopez del Amo JM, Gruning BA, Wang Q, Schmidt MR, Lurz R, Anwyl R, Schnoegl S, Fandrich M, Frank RF, Reif B, Gunther S, Walsh DM, Wanker EE (2012) Small-molecule conversion of toxic oligomers

©2013 European Molecular Biology Organization

to nontoxic beta-sheet-rich amyloid fibrils. *Nat Chem Biol* **8:** 93–101

Binder LI, Frankfurter A, Rebhun LI (1986) Differential localization of MAP-2 and tau in mammalian neurons *in situ*. *Ann NY Acad Sci* **466:** 145–166

Braak E, Braak H, Mandelkow EM (1994) A sequence of cytoskeleton changes related to the formation of neurofibrillary tangles and neuropil threads. *Acta Neuropathol* **87:** 554–567

Braak H, Braak E (1991) Neuropathological stageing of Alzheimer-related changes. *Acta Neuropathol* **82:** 239–259

Braak H, Del Tredici K (2011) The pathological process underlying Alzheimer's disease in individuals under thirty. *Acta Neuropathol* **121:** 171–181

Bullmann T, Holzer M, Mori H, Arendt T (2009) Pattern of tau isoforms expression during development *in vivo*. *Int J Dev Neurosci* **27:** 591–597

Conde C, Caceres A (2009) Microtubule assembly, organization and dynamics in axons and dendrites. *Nat Rev* **10:** 319–332

Dawson HN, Cantillana V, Jansen M, Wang H, Vitek MP, Wilcock DM, Lynch JR, Laskowitz DT (2010) Loss of tau elicits axonal degeneration in a mouse model of Alzheimer's disease. *Neuroscience* **169:** 516–531

Dawson HN, Ferreira A, Eyster MV, Ghoshal N, Binder LI, Vitek MP (2001) Inhibition of neuronal maturation in primary hippocampal neurons from tau deficient mice. *J Cell Sci* **114:** 1179–1187

Drewes G, Ebneth A, Preuss U, Mandelkow EM, Mandelkow E (1997) MARK, a novel family of protein kinases that phosphorylate microtubule-associated proteins and trigger microtubule disruption. *Cell* **89:** 297–308

Ebneth A, Godemann R, Stamer K, Illenberger S, Trinczek B, Mandelkow E (1998) Overexpression of tau protein inhibits kinesin-dependent trafficking of vesicles, mitochondria, and endoplasmic reticulum: implications for Alzheimer's disease. *J Cell Biol* **143:** 777–794

Fulga TA, Elson-Schwab I, Khurana V, Steinhilb ML, Spires TL, Hyman BT, Feany MB (2007) Abnormal bundling and accumulation of F-actin mediates tau-induced neuronal degeneration *in vivo*. *Nat Cell Biol* **9:** 139–148

Gustke N, Trinczek B, Biernat J, Mandelkow EM, Mandelkow E (1994) Domains of tau protein and interactions with microtubules. *Biochemistry* **33:** 9511–9522

Haass C, Selkoe DJ (2007) Soluble protein oligomers in neurodegeneration: lessons from the Alzheimer's amyloid beta-peptide. *Nat Rev* **8:** 101–112

Harada A, Oguchi K, Okabe S, Kuno J, Terada S, Ohshima T, Sato-Yoshitake R, Takei Y, Noda T, Hirokawa N (1994) Altered microtubule organization in small-calibre axons of mice lacking tau protein. *Nature* **369:** 488–491

Hayashi K, Suzuki A, Hirai S, Kurihara Y, Hoogenraad CC, Ohno S (2011) Maintenance of dendritic spine morphology by partitioning-defective 1b through regulation of microtubule growth. *J Neurosci* **31:** 12094–12103

Higley MJ, Sabatini BL (2008) Calcium signaling in dendrites and spines: practical and functional considerations. *Neuron* **59:** 902–913

Hoogenraad CC, Bradke F (2009) Control of neuronal polarity and plasticity–a renaissance for microtubules? *Trends Cell Biol* **19:** 669–676

Hoover BR, Reed MN, Su J, Penrod RD, Kotilinek LA, Grant MK, Pitstick R, Carlson GA, Lanier LM, Yuan LL, Ashe KH, Liao D (2010) Tau mislocalization to dendritic spines mediates synaptic dysfunction independently of neurodegeneration. *Neuron* **68:** 1067–1081

Ishihara T, Hong M, Zhang B, Nakagawa Y, Lee MK, Trojanowski JQ, Lee VM (1999) Age-dependent emergence and progression of a tauopathy in transgenic mice overexpressing the shortest human tau isoform. *Neuron* **24:** 751–762

Ittner LM, Ke YD, Delerue F, Bi M, Gladbach A, van Eersel J, Wolfing H, Chieng BC, Christie MJ, Napier IA, Eckert A, Staufenbiel M, Hardeman E, Gotz J (2010) Dendritic function of tau mediates amyloid-beta toxicity in Alzheimer's disease mouse models. *Cell* **142:** 387–397

Iwaya N, Akiyama K, Goda N, Tenno T, Fujiwara Y, Hamada D, Ikura T, Shirakawa M, Hiroaki H (2012) Effect of Ca(2+) on the microtubule-severing enzyme p60-katanin: insight into the substrate-dependent activation mechanism. *FEBS J* **279:** 1339–1352

Janke C, Kneussel M (2010) Tubulin post-translational modifications: encoding functions on the neuronal microtubule cytoskeleton. *Trends Neurosci* **33:** 362–372

Jaworski J, Kapitein LC, Gouveia SM, Dortland BR, Wulf PS, Grigoriev I, Camera P, Spangler SA, Di Stefano P, Demmers J, Krugers H, Defilippi P, Akhmanova A, Hoogenraad CC (2009) Dynamic microtubules regulate dendritic spine morphology and synaptic plasticity. *Neuron* **61:** 85–100

Kampers T, Friedhoff P, Biernat J, Mandelkow EM, Mandelkow E (1996) RNA stimulates aggregation of microtubule-associated protein tau into Alzheimer-like paired helical filaments. *FEBS Lett* **399:** 344–349

Kanai Y, Hirokawa N (1995) Sorting mechanisms of tau and MAP2 in neurons: suppressed axonal transit of MAP2 and locally regulated microtubule binding. *Neuron* **14:** 421–432

Kang JE, Lim MM, Bateman RJ, Lee JJ, Smyth LP, Cirrito JR, Fujiki N, Nishino S, Holtzman DM (2009) Amyloid-beta dynamics are regulated by orexin and the sleep-wake cycle. *Science (New York, NY)* **326:** 1005–1007

Karran E, Mercken M, De Strooper B (2011) The amyloid cascade hypothesis for Alzheimer's disease: an appraisal for the development of therapeutics. *Nat Rev Drug Discov* **10:** 698–712

King ME, Kan HM, Baas PW, Erisir A, Glabe CG, Bloom GS (2006) Tau-dependent microtubule disassembly initiated by prefibrillar beta-amyloid. *J Cell Biol* **175:** 541–546

Klein WL (2006) Synaptic targeting by Abeta oligomers (ADDLS) as a basis for memory loss in early Alzheimer's disease. *Alzheimers Dement* **2:** 43–55

Konzack S, Thies E, Marx A, Mandelkow EM, Mandelkow E (2007) Swimming against the tide: mobility of the microtubule-associated protein tau in neurons. *J Neurosci* **27:** 9916–9927

Kuperstein I, Broersen K, Benilova I, Rozenski J, Jonckheere W, Debulpaep M, Vandersteen A, Segers-Nolten I, Van Der Werf K, Subramaniam V, Braeken D, Callewaert G, Bartic C, D'Hooge R, Martins IC, Rousseau F, Schymkowitz J, De Strooper B (2010) Neurotoxicity of Alzheimer's disease Abeta peptides is induced by small changes in the Abeta42 to Abeta40 ratio. *EMBO J* **29:** 3408–3420

Lacroix B, van Dijk J, Gold ND, Guizetti J, Aldrian-Herrada G, Rogowski K, Gerlich DW, Janke C (2010) Tubulin polyglutamylation stimulates spastin-mediated microtubule severing. *J Cell Biol* **189:** 945–954

LaFerla FM (2002) Calcium dyshomeostasis and intracellular signalling in Alzheimer's disease. *Nat Rev* **3:** 862–872

Lauren J, Gimbel DA, Nygaard HB, Gilbert JW, Strittmatter SM (2009) Cellular prion protein mediates impairment of synaptic plasticity by amyloid-beta oligomers. *Nature* **457:** 1128–1132

Lei P, Ayton S, Finkelstein DI, Spoerri L, Ciccotosto GD, Wright DK, Wong BX, Adlard PA, Cherny RA, Lam LQ, Roberts BR, Volitakis I, Egan GF, McLean CA, Cappai R, Duce JA, Bush AI (2012) Tau deficiency induces parkinsonism with dementia by impairing APP-mediated iron export. *Nat Med* **18:** 291–295

Li X, Kumar Y, Zempel H, Mandelkow EM, Biernat J, Mandelkow E (2011) Novel diffusion barrier for axonal retention of Tau in neurons and its failure in neurodegeneration. *EMBO J* **30:** 4825–4837

Mandelkow EM, Mandelkow E (2012) Biochemistry and cell biology of tau protein in neurofibrillary degeneration. *Cold Spring Harb Perspect Med* **2:** a006247

Mandell JW, Banker GA (1995) The microtubule cytoskeleton and the development of neuronal polarity. *Neurobiol Aging* **16:** 229–237, discussion 238

Matenia D, Griesshaber B, Li XY, Thiessen A, Johne C, Jiao J, Mandelkow E, Mandelkow EM (2005) PAK5 kinase is an inhibitor of MARK/Par-1, which leads to stable microtubules and dynamic actin. *Mol Biol Cell* **16:** 4410–4422

Matenia D, Mandelkow EM (2009) The tau of MARK: a polarized view of the cytoskeleton. *Trends Biochem Sci* **34:** 332–342

Morris M, Maeda S, Vossel K, Mucke L (2011) The many faces of tau. *Neuron* **70:** 410–426

Mucke L, Selkoe DJ (2012) Neurotoxicity of amyloid beta-protein: synaptic and network dysfunction. *Cold Spring Harb Perspect Med* **2:** a006338

 ©2013 European Molecular Biology Organization

Nakata T, Niwa S, Okada Y, Perez F, Hirokawa N (2011) Preferential binding of a kinesin-1 motor to GTP-tubulin-rich microtubules underlies polarized vesicle transport. *J Cell Biol* **194:** 245–255

Palop JJ, Mucke L (2009) Epilepsy and cognitive impairments in Alzheimer disease. *Arch Neurol* **66:** 435–440

Qiang L, Yu W, Andreadis A, Luo M, Baas PW (2006) Tau protects microtubules in the axon from severing by katanin. *J Neurosci* **26:** 3120–3129

Rapoport M, Dawson HN, Binder LI, Vitek MP, Ferreira A (2002) Tau is essential to beta -amyloid-induced neurotoxicity. *Proc Natl Acad Sci USA* **99:** 6364–6369

Riano E, Martignoni M, Mancuso G, Cartelli D, Crippa F, Toldo I, Siciliano G, Di Bella D, Taroni F, Bassi MT, Cappelletti G, Rugarli EI (2009) Pleiotropic effects of spastin on neurite growth depending on expression levels. *J Neurochem* **108:** 1277–1288

Roberson ED, Scearce-Levie K, Palop JJ, Yan F, Cheng IH, Wu T, Gerstein H, Yu GQ, Mucke L (2007) Reducing endogenous tau ameliorates amyloid beta-induced deficits in an Alzheimer's disease mouse model. *Science (New York, NY)* **316:** 750–754

Roll-Mecak A, McNally FJ (2010) Microtubule-severing enzymes. *Curr Opin Cell Biol* **22:** 96–103

Rui Y, Li R, Liu Y, Zhu S, Yu X, Sheng Z, Xie Z (2006) Acute effect of beta amyloid on synchronized spontaneous Ca2 + oscillations in cultured hippocampal networks. *Cell Biol Int* **30:** 733–740

Salinas S, Carazo-Salas RE, Proukakis C, Cooper JM, Weston AE, Schiavo G, Warner TT (2005) Human spastin has multiple microtubule-related functions. *J Neurochem* **95:** 1411–1420

Sapir T, Shmueli A, Levy T, Timm T, Elbaum M, Mandelkow EM, Reiner O (2008) Antagonistic effects of doublecortin and MARK2/Par-1 in the developing cerebral cortex. *J Neurosci* **28:** 13008–13013

Sarkar M, Kuret J, Lee G (2008) Two motifs within the tau microtubule-binding domain mediate its association with the hsc70 molecular chaperone. *J Neurosci Res* **86:** 2763–2773

Schliwa M, Euteneuer U, Bulinski JC, Izant JG (1981) Calcium lability of cytoplasmic microtubules and its modulation by microtubule-associated proteins. *Proc Natl Acad Sci USA* **78:** 1037–1041

Shankar GM, Bloodgood BL, Townsend M, Walsh DM, Selkoe DJ, Sabatini BL (2007) Natural oligomers of the Alzheimer amyloid-beta protein induce reversible synapse loss by modulating an NMDA-type glutamate receptor-dependent signaling pathway. *J Neurosci* **27:** 2866–2875

Sharma VM, Litersky JM, Bhaskar K, Lee G (2007) Tau impacts on growth-factor-stimulated actin remodeling. *J Cell Sci* **120:** 748–757

Snyder EM, Nong Y, Almeida CG, Paul S, Moran T, Choi EY, Nairn AC, Salter MW, Lombroso PJ, Gouras GK, Greengard P (2005) Regulation of NMDA receptor trafficking by amyloid-beta. *Nat Neurosci* **8:** 1051–1058

Spires-Jones TL, Stoothoff WH, de Calignon A, Jones PB, Hyman BT (2009) Tau pathophysiology in neurodegeneration: a tangled issue. *Trends Neurosci* **32:** 150–159

Stamer K, Vogel R, Thies E, Mandelkow E, Mandelkow EM (2002) Tau blocks traffic of organelles, neurofilaments, and APP vesicles in neurons and enhances oxidative stress. *J Cell Biol* **156:** 1051–1063

Sudo H, Baas PW (2010) Strategies for diminishing katanin-based loss of microtubules in tauopathic neurodegenerative diseases. *Hum Mol Genet* **20:** 763–778

Sudo H, Maru Y (2007) LAPSER1 is a putative cytokinetic tumor suppressor that shows the same centrosome and midbody subcellular localization pattern as p80 katanin. *FASEB J* **21:** 2086–2100

Sultan A, Nesslany F, Violet M, Begard S, Loyens A, Talahari S, Mansuroglu Z, Marzin D, Sergeant N, Humez S, Colin M, Bonnefoy E, Buee L, Galas MC (2011) Nuclear tau, a key player in neuronal DNA protection. *J Biol Chem* **286:** 4566–4575

Sydow A, Van der Jeugd A, Zheng F, Ahmed T, Balschun D, Petrova O, Drexler D, Zhou L, Rune G, Mandelkow E, D'Hooge R, Alzheimer C, Mandelkow EM (2011) Tau-induced defects in synaptic plasticity, learning, and memory are reversible in transgenic mice after switching off the toxic Tau mutant. *J Neurosci* **31:** 2511–2525

Thies E, Mandelkow EM (2007) Missorting of tau in neurons causes degeneration of synapses that can be rescued by the kinase MARK2/Par-1. *J Neurosci* **27:** 2896–2907

Timm T, von Kries JP, Li X, Zempel H, Mandelkow E, Mandelkow EM (2011) Microtubule affinity regulating kinase activity in living neurons was examined by a genetically encoded fluorescence resonance energy transfer/fluorescence lifetime imaging-based biosensor: inhibitors with therapeutic potential. *J Biol Chem* **286:** 41711–41722

Van der Jeugd A, Hochgrafe K, Ahmed T, Decker JM, Sydow A, Hofmann A, Wu D, Messing L, Balschun D, D'Hooge R, Mandelkow EM (2012) Cognitive defects are reversible in inducible mice expressing pro-aggregant full-length human Tau. *Acta Neuropathol* **123:** 787–805

Wang X, Schwarz TL (2009) The mechanism of Ca^{2+}-dependent regulation of kinesin-mediated mitochondrial motility. *Cell* **136:** 163–174

Wei W, Nguyen LN, Kessels HW, Hagiwara H, Sisodia S, Malinow R (2010) Amyloid beta from axons and dendrites reduces local spine number and plasticity. *Nat Neurosci* **13:** 190–196

Whiteman IT, Gervasio OL, Cullen KM, Guillemin GJ, Jeong EV, Witting PK, Antao ST, Minamide LS, Bamburg JR, Goldsbury C (2009) Activated actin-depolymerizing factor/cofilin sequesters phosphorylated microtubule-associated protein during the assembly of alzheimer-like neuritic cytoskeletal striations. *J Neurosci* **29:** 12994–13005

Williamson R, Usardi A, Hanger DP, Anderton BH (2008) Membrane-bound beta-amyloid oligomers are recruited into lipid rafts by a fyn-dependent mechanism. *FASEB J* **22:** 1552–1559

Wogulis M, Wright S, Cunningham D, Chilcote T, Powell K, Rydel RE (2005) Nucleation-dependent polymerization is an essential component of amyloid-mediated neuronal cell death. *J Neurosci* **25:** 1071–1080

Ye B, Kim JH, Yang L, McLachlan I, Younger S, Jan LY, Jan YN (2011) Differential regulation of dendritic and axonal development by the novel Kruppel-like factor Dar1. *J Neurosci* **31:** 3309–3319

Yu W, Solowska JM, Qiang L, Karabay A, Baird D, Baas PW (2005) Regulation of microtubule severing by katanin subunits during neuronal development. *J Neurosci* **25:** 5573–5583

Zempel H, Mandelkow EM (2012) Linking amyloid-beta and tau: amyloid-beta induced synaptic dysfunction via local wreckage of the neuronal cytoskeleton. *Neurodegener Dis* **10:** 64–72

Zempel H, Thies E, Mandelkow E, Mandelkow EM (2010) Abeta oligomers cause localized Ca(2 +) elevation, missorting of endogenous Tau into dendrites, Tau phosphorylation, and destruction of microtubules and spines. *J Neurosci* **30:** 11938–11950

Zhang B, Carroll J, Trojanowski JQ, Yao Y, Iba M, Potuzak JS, Hogan AM, Xie SX, Ballatore C, Smith 3rd AB, Lee VM, Brunden KR (2012) The microtubule-stabilizing agent, epothilone D, reduces axonal dysfunction, neurotoxicity, cognitive deficits, and Alzheimer-like pathology in an interventional study with aged tau transgenic mice. *J Neurosci* **32:** 3601–3611

©2013 European Molecular Biology Organization